

# Environmentally Friendly Thermoelectric Materials: High Performance from Inorganic Components with Low Toxicity and Abundance in the Earth

Olga Caballero-Calero, José R. Ares, and Marisol Martín-González\*

This review article gives an overview of the recent research directions in eco-friendly, non-toxic, and earth-abundant thermoelectric materials. It covers materials such as sulfides, tetrahedrites, earth-abundant oxides, silicides, copper iodine, Half-Heusler intermetallic compounds, nitrides, and other environmentally friendly thermoelectrics. In all cases, their history, structure, general characteristics, thermoelectric properties, synthesis methods, and related thermoelectric applications are compiled. It is also shown that they are starting to be an excellent alternative for producing cost-effective, sustainable, and non-toxic thermoelectric generators. This review does not try to include all possible materials, but to show that there are high  $zT$  thermoelectric materials that are starting to be an excellent alternative for producing cost-effective, sustainable, and non-toxic thermoelectric generators.

## 1. Introduction

Today, we are becoming more and more aware of the need for clean, renewable energy sources to preserve our environment. On the one hand, the energy demand is growing, and on the other hand, the supply of fossil fuels is limited, and climate change is a reality. Currently, most of the energy production/conversion methods are based on thermal processes that generate an enormous amount of residual/waste heat to be released into the environment.<sup>[1]</sup> Using this waste heat to produce

energy would improve the efficiency of all these processes. In this context, thermoelectric devices provide a unique opportunity with significant advantages relative to other types of conversion, such as durability (no moving parts or fluids inside the generator), noise-free, low maintenance, modulability, and their applicability at different scales (from microdevices to large spaces to produce kilowatts), etc.<sup>[2]</sup> The implementation of thermoelectric generators has been limited for many years because of their low efficiency and high cost. There are examples of these limited applications like in space missions such as the Voyager, Apollo, Curiosity, etc.<sup>[3]</sup> when reliability is mandatory. Other niche applications with products that are being sold


are, for instance, the powering of smartwatches with wasted heat from the human body<sup>[4]</sup> or the obtainment of electricity from the heat produced in wood stoves,<sup>[5]</sup> among others.<sup>[6]</sup>

The vast majority of commercial thermoelectric devices are based on heavy elements like Bismuth and Tellurium. Which, according to **Figure 1a** are among the rarest elements in the Earth's crust on the order of noble metals (like Au, Pt...) or even less abundant. Therefore, they are more expensive to manufacture. Other thermoelectrics with high figure of merit can be based on moderately toxic elements (or even highly toxic elements, like Pb, which is part of some of the best performing thermoelectrics but is banned in the EU). The toxicity of the elements in the Periodic Table is shown in **Figure 1b**. Therefore, although the use of less abundant or toxic elements is of interest at the research level because they allow us to understand and underpin the physics behind thermoelectricity and develop new strategies to improve them. However, to develop safe and widespread thermoelectric applications the use of less abundant or toxic elements does not seem to be the best option.

Traditionally, the research in the field of thermoelectric materials has focused on improving the adimensional figure-of-merit,  $zT$ , which is related to the energy conversion efficiency of thermoelectric materials. This figure of merit can be expressed as  $zT = S^2 \cdot \sigma \cdot T \cdot \kappa^{-1}$ , where  $S$  is the Seebeck coefficient,  $\sigma$  the electrical conductivity,  $T$  the absolute temperature, and  $\kappa$  the thermal conductivity. In recent years,  $zT$  values higher than 2 have been obtained at the laboratory level, implying efficiency values above 10% in proof-of-concept prototypes.<sup>[7]</sup> Despite the enormous effort being made to reach these values, they are still

Dr. O. Caballero-Calero, Prof. M. Martín-González  
 Instituto de Micro y Nanotecnología  
 IMN-CNM  
 CSIC (CEI UAM+CSIC) Isaac Newton  
 8, Tres Cantos, Madrid E-28760, Spain  
 E-mail: Marisol.martin@csic.es

Dr. J. R. Ares  
 MIRE-group  
 Dpto. de Física de Materiales  
 UAM  
 Cantoblanco  
 Madrid E-28049, Spain

 The ORCID identification number(s) for the author(s) of this article can be found under <https://doi.org/10.1002/adsu.202100095>.

© 2021 The Authors. Advanced Sustainable Systems published by Wiley-VCH GmbH. This is an open access article under the terms of the Creative Commons Attribution-NonCommercial License, which permits use, distribution and reproduction in any medium, provided the original work is properly cited and is not used for commercial purposes.

DOI: 10.1002/adsu.202100095

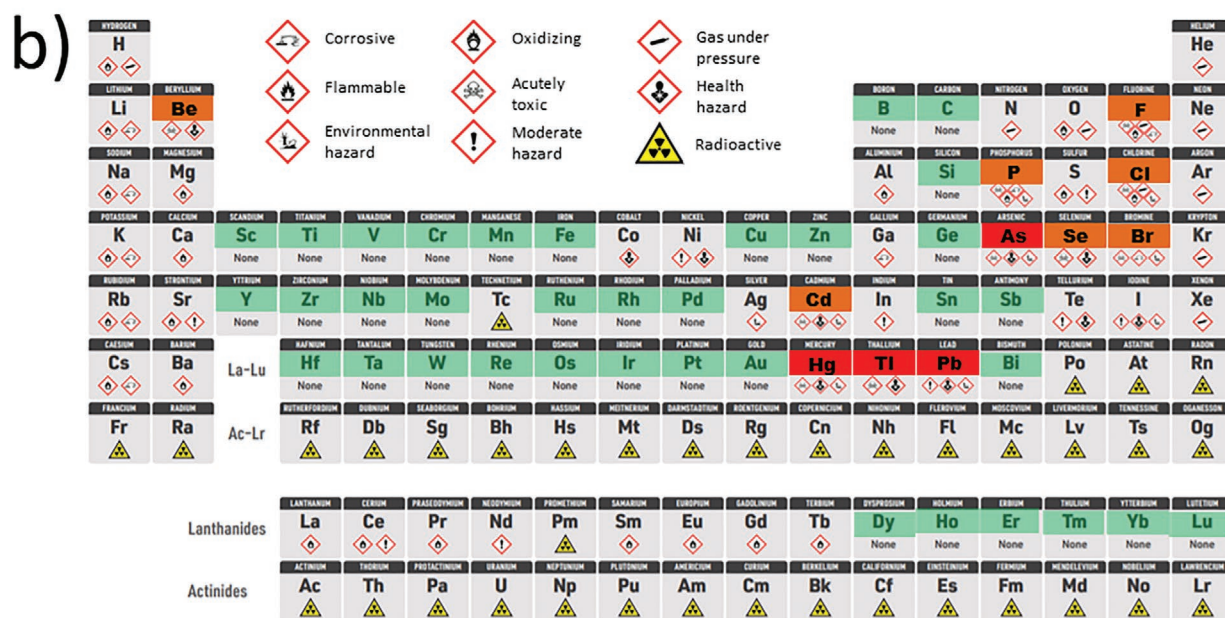
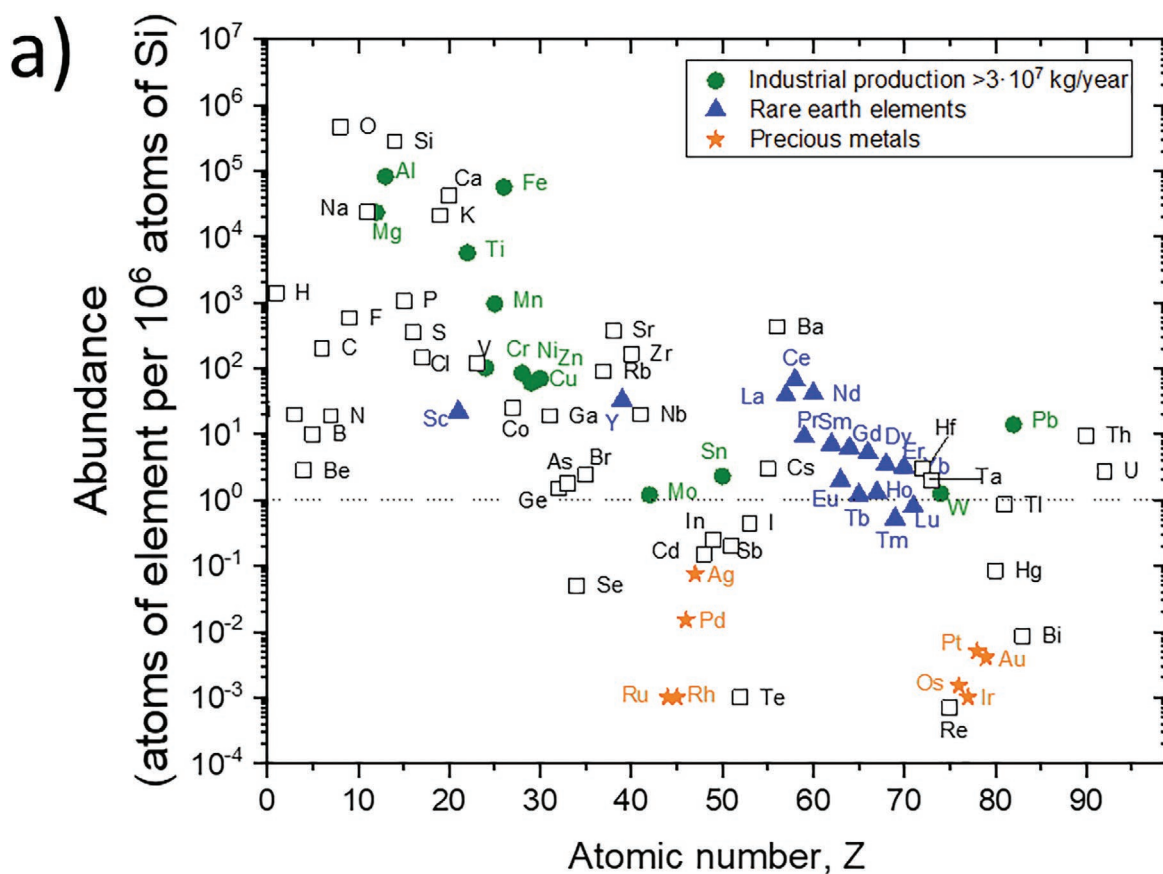


**Figure 1.** a) The abundance of individual elements relative to their atomic number, based on data extracted from Ref. [11]. Elements that are produced at the industrial level are marked with a green circle, rare earth elements with a blue triangle, and precious metals with an orange star. A dashed line has been added to mark the abundance corresponding to 1 atom of a certain element per  $10^6$  atoms of Si. Elements over the dashed line may be considered as Earth-abundant. b) Periodic table with toxic elements according to SDS datasheets (Reproduced with permission,<sup>[233]</sup> Copyright 2019, Andy Bruning). The non-toxic elements are colored in green, whereas the moderately hazardous elements are colored in orange and the four most dangerous are colored in red. Nevertheless, some of the non-toxic elements may be flammable when used as nanoparticles in air.

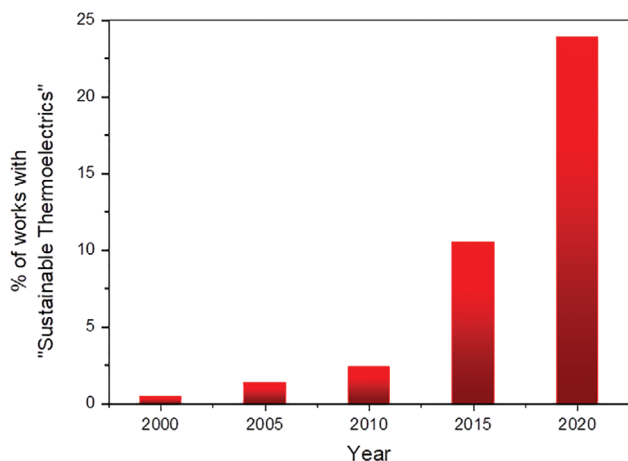


**Figure 2.** The percentage of published articles including the word *sustainable* in the KEYWORD field among all published articles in the same time-span including the word *thermoelectric* as KEYWORD. Data derived from Web of Science. Notice the exponential trend, which marks the importance that sustainability has in this field: nowadays more than 25% of the articles match with the search criteria, while 20 years ago this percentage is hardly 1%.

far from those required by the industry to make their commercialization profitable because of the high cost of raw materials.

These improvements have been frequently based on the reduction of the thermal conductivity of those compounds by using different approaches (nanocrystallization, the introduction of defects...), but most are based on the initial use of heavy scarce elements to reduce the thermal conductivity of these materials. This is because the total thermal conductivity ( $k$ ) depends on two components, the electronic component ( $k_e$ ) and the phononic component ( $k_{ph}$ ). As  $k_e$  is related to the electrical conductivity by the Wiedemann–Franz law, the strategy of reducing the electronic part of the thermal conductivity cannot be adopted. This would also decrease the power factor ( $S^2 \cdot \sigma$ ). This means that to reduce the total thermal conductivity only the strategy of reducing  $k_{ph}$  can be adopted. The  $k_{ph} = 1/3 \cdot C_e \cdot v \cdot l$ , where  $C_e$  is the specific heat capacity,  $v$  is the velocity of sound in the solid, and  $l$  is the phonon mean free path. Considering that thermoelectric materials are normally desirable to be used for applications at room temperature and above, the heat capacity  $C_e$  is governed by the Dulong–Petit law where  $C_e \approx 3 \cdot R$  (where  $R$  is the universal gas constant and  $3 \cdot R$  is about 25 J/K). Consequently, the specific heat cannot be significantly modified. This means that the factors that can be set to alter the  $k_{ph}$  are mainly the speed of sound in the solid, and the phonon mean free path. The research in the scarce elements has drawn a more in-depth understanding of the physics underlying thermoelectricity and, although it is not yet understood, that are some general conclusions that are nowadays assumed by the community, for example, that it is possible to reduce the sound velocity in a solid by heavy elements and to reduce the phonon mean free path nanostructuring is one of the main options.<sup>[8–10]</sup>

But surprisingly enough, when taking into account this previous point of view, good thermoelectric materials can also be found in elements with a lower atomic number which are also among the most abundant in earth crust. These abundant, efficient, and non-toxic thermoelectric materials have been the focus of recent research by the thermoelectric community, as

shown in **Figure 2**. To this end, we will attempt to summarize some of the most studied thermoelectric materials based on these characteristics. Lately, there have been interesting and thorough review articles focused on the latest developments of thermoelectric materials (see for instance Refs. [7,12–14]) or more on different families of materials (such as sulfides,<sup>[15,16]</sup> oxides,<sup>[17,18]</sup> chalcogenides,<sup>[19–21]</sup> graphene-based,<sup>[22]</sup> silicon,<sup>[23]</sup> polymers or composites<sup>[24,25]</sup>) or different structures (such as nanostructured materials,<sup>[9,10,26,27]</sup> layered materials,<sup>[28]</sup> 2D materials<sup>[29,30]</sup>) or a variety of applications (wearable thermoelectric harvesters,<sup>[31]</sup> or others<sup>[32–34]</sup>). In our case, we will extract from the different families of materials and applications those which are based on abundant-earth elements, and also in the modifications that have produced and enhancement of their thermoelectric properties avoiding the use of hazardous or scarce elements. Among these, we will review not only their thermoelectric properties, but also other aspects like their history, cost, thermal, chemical, and mechanical stability, fabrication routes, and possible scalability, which are also important for making this technology viable and widely used.

Among the earth-abundant thermoelectrics for commercial applications, silicon and silicon-based materials stand out as easily implemented in industrial applications, given the high level of development of the microelectronics field. Nevertheless, there are some recent reviews focused exclusively on these materials,<sup>[35–37]</sup> and we will focus our review on other less reviewed ones. In some cases, their thermoelectric performance is not outstanding when compared to other more traditional scarce thermoelectric materials, but even though not reaching the highest performance possible, many applications require that the materials are produced in an inexpensive way and at a large scale. In this work, we will review their history and the best performing thermoelectric materials composed of abundant earth elements reported to date. We will consider earth-abundant elements those which have over 1 atom of the element per million atoms of Si in the earth crust (see Figure 1) and we will try to focus on non-toxic elements too (according to Figure 1). We will start with sulfides, which although having lower efficiency than the most used thermoelectric materials for room temperature applications, are abundant, non-toxic and there is a high variety of compounds that exhibit interesting properties that are being studied nowadays for thermoelectric applications. Then, we will turn to tetrahedrites, which are sulfosalts naturally present on the earth's crust and which have shown huge figures of merit, in the order of 1, for different doping or nanostructures. Oxides and silicides also form a very interesting group with promising properties for high-temperature applications, and as a result, they will be also considered. Although all these families of materials have more modest thermoelectric performances than the more widely studied traditional thermoelectric materials, they have the advantage of being based on earth-abundant elements.

Throughout this review, it will be shown that there is still plenty of room for research in this area. In fact, **Figure 3** shows the huge impact of those compounds on the thermoelectric figure of merit during the last 10 years. Whereas tetrahedrites are able to provide  $zT$  near to 1 at RT, an extensive family of sulfides is starting to be synthesized and thermoelectrically characterized, exhibiting very high  $zT$  values. Those results indicate that both families are very promising to find an efficient environmentally friendly compound able to work at

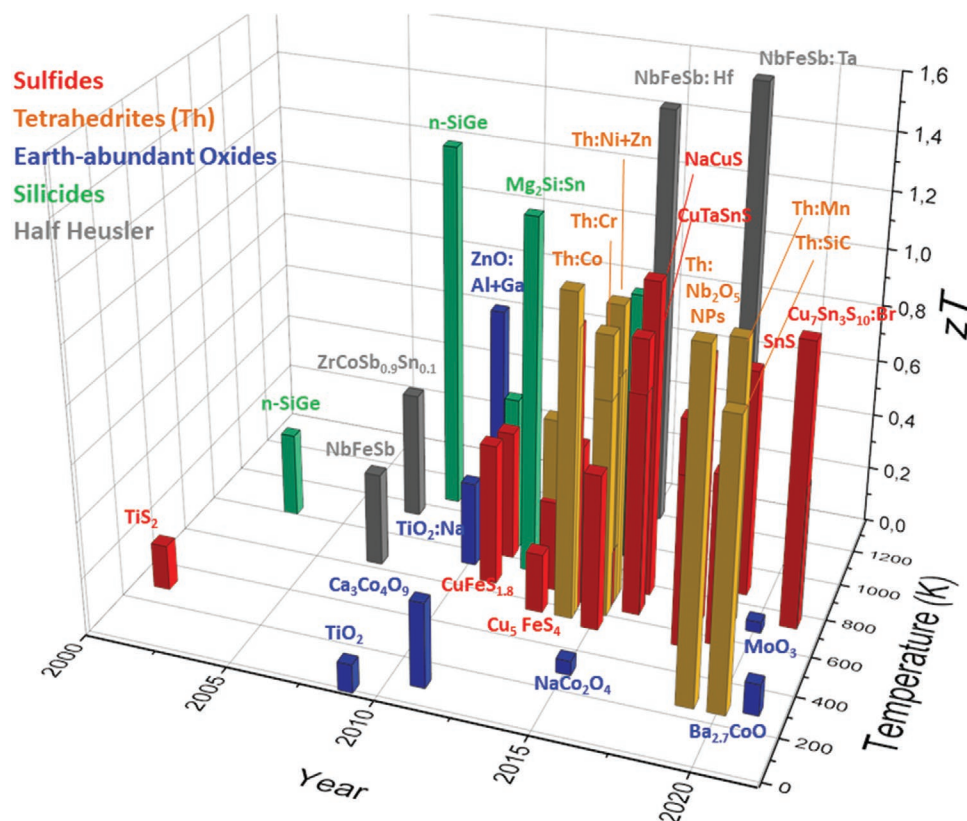


**Figure 3.** Evolution of the  $zT$  obtained for different materials for different temperatures in recent years (from 2002 to today, 2021), based on the data analyzed in this article. The different materials are sulfides (red), tetrahedrites (yellow), earth-abundant oxides (blue), silicides (green), and HH (grey).

room temperature. Concerning moderate and high temperatures, research has been focused on Half-Heusler (HH) compounds, oxides, and silicides, which show the highest figure of merit. Finally, we will review some other materials which exhibit certain properties that make them good candidates for thermoelectric applications, while being based on earth-abundant and non-toxic elements, such as copper iodide, or nitrides. After giving a perspective of the state of the art on all those earth-abundant materials for thermoelectric applications, we hope that we will have showed also the interest and possibilities that the research of thermoelectric applications based on sustainable and environmentally-friendly materials offer nowadays.

## 2. Sulfides

In the thermoelectric landscape, tellurides and selenides have formed the archetypal thermoelectric compounds for more than half a century. The reasons are attributed to their easy synthesis, moderate  $zT$ , and prices, and well-established implementation.<sup>[3]</sup> However, because of environmental reasons and scarcity, they should be replaced in the future if the plan is to have widespread applications. One possible way to accomplish this is to consider the sulfides group due to their chemical and structural resemblance to tellurides and selenides. They have lower figures of merit than their scarce counterparts because the mass of the sulfur atom is lighter than that of selenium or tellurium, as well as most of them also exhibit an intrinsically very high or very low charge carrier concentration (extreme

concentrations normally due to defects). However, they have recently given considerable attention to the thermoelectric landscape because of their wide range of compounds, easy synthesis, low toxicity, and abundance.

Sulfides are strongly linked to the origin of thermoelectricity. Original works from T.J. Seebeck in the 19th century<sup>[38]</sup> or in the 1950s, M. Telkes<sup>[39]</sup> measured the thermoelectric properties (primarily electrical conductivity and Seebeck coefficient) of several sulfides in mineral form. Consequently, minerals such as chalcocite ( $\text{Cu}_2\text{S}$ ) ( $S \approx 54$  to  $327 \mu\text{V}\cdot\text{K}^{-1}$ ), galena ( $\text{PbS}$ ) ( $S \approx -290 \mu\text{V}\cdot\text{K}^{-1}$  and between  $150$  and  $340 \mu\text{V}\cdot\text{K}^{-1}$  with “n” and “p” type conductivities, respectively), chalcopyrite ( $\text{CuFeS}_2$ ) ( $S \approx -280$  to  $-425 \mu\text{V}\cdot\text{K}^{-1}$ ) and  $\text{FeS}_2$  in pyrite form ( $S = -344$  to  $524 \mu\text{V}\cdot\text{K}^{-1}$ ) and in marcasite form ( $S \approx 280 \mu\text{V}\cdot\text{K}^{-1}$ ) were measured. For example, chalcocite has a power factor close to  $\approx 1.2 \times 10^{-4} \text{ W}\cdot\text{m}^{-1}\cdot\text{K}^{-2}$ , a similar value to those given by galena ( $\text{PbS}$ ).

Pyrite itself, (synthesized mainly in bulk), has been investigated as an archetypal thermoelectric sulfide. It has relatively high Seebeck coefficient values ( $S \approx 300 \mu\text{V}\cdot\text{K}^{-1}$  at  $300 \text{ K}$ ) but moderate thermal conductivity ( $26 \text{ W}\cdot\text{m}^{-1}\cdot\text{K}^{-1}$  at RT and  $5 \text{ W}\cdot\text{m}^{-1}\cdot\text{K}^{-1}$  at  $270 \text{ }^\circ\text{C}$ ) and electrical conductivity ( $10$  to  $10^3 \text{ S}\cdot\text{m}^{-1}$ ) leading to modest values of the figure of merit, that is, from  $zT \approx 0.004$  at room temperature to  $zT \approx 0.07$  at  $543 \text{ K}$ .<sup>[40]</sup> However, recent ab initio calculations indicate that the figure of merit value of  $\text{FeS}_2$  can reach  $zT \approx 0.32$  at  $700 \text{ K}$  by p-type doping.<sup>[41]</sup> With these values, an efficiency of 4% (obtained considering a temperature difference of  $300 \text{ }^\circ\text{C}$  and the cold focus at room temperature) could be obtained, which is close to the

≈6% shown by Bi<sub>2</sub>Te<sub>3</sub>. However, considering that the cost of extracted pyrite (≈1 \$ kg<sup>-1</sup>) is much lower than that of Bi<sub>2</sub>Te<sub>3</sub> (50 \$ kg<sup>-1</sup>), together with its low toxicity, it has led to a renewed interest in improving its thermoelectric properties by different means, that, nanostructuration, dimensional effects, or doping. For instance, their power factor has recently been doubled by doping with cobalt.<sup>[42]</sup>

In addition to the “classical” pyrite, many “antique” metal sulfides have recently emerged as promising thermoelectric materials. It is remarkable, the case of Cu<sub>2-x</sub>S that shows very high values of figure-of-merit, that is, ≈1.4 for Cu<sub>1.98</sub>S and ≈1.7 for Cu<sub>1.97</sub>S at a temperature of 1000 K primarily due to its extremely low thermal conductivity ( $\kappa \approx 0.6 \text{ W} \cdot \text{m}^{-1} \cdot \text{K}^{-1}$ <sup>[43]</sup>) induced by its special properties. Also, Cu<sub>1.8</sub>S has shown values of  $zT$  of 0.5 at 673 K when consolidated at high temperatures (973 K, by Spark Plasma Sintering (SPS)), because it produces a lower thermal conductivity.<sup>[44]</sup> Moreover, sodium doping showed an improvement in the figure of merit, reaching  $zT$  of 1.1 at 773 K for the Na<sub>0.01</sub>Cu<sub>1.8</sub>S composition.<sup>[45]</sup> Another way of reducing the thermal conductivity in the material is to fabricate nanocomposites of Cu<sub>1.8</sub>S with nanoparticles of graphene, for instance,<sup>[46]</sup> which increases the scattering at the nanocomposite interfaces. This sulfide exhibits a superionic conductivity above a moderate temperature (thanks to an order/disorder transition) which is based on the coexistence of two crystal lattices: a rigid lattice and a disordered lattice (reviews on Cu based thermoelectric materials can be found in references<sup>[20,47]</sup>). Whereas the disorder sublattice can strongly scatter phonons (and therefore, reduce the thermal conductivity), the rigid lattice contributes to the electrical properties by liquid-like ionic conductivities (values  $1 \text{ S} \cdot \text{cm}^{-1}$ ).<sup>[37]</sup>

One of the main problems of copper sulfides is the Cu-ion diffusion, which turns into stability problems. Therefore, an alternative is to look at ternary compounds. For instance, the n-type mineral chalcopyrite, CuFeS<sub>2</sub>, has greater stability, but also, rather modest thermoelectric properties.<sup>[48,49]</sup> However, theoretical calculations predict an increase of  $zT$  to 0.8 at 700 K if the grain size is reduced to 20 nm and the material is properly doped.<sup>[50]</sup> This has been tried by partial substitution of copper with iron, for example, where values of  $zT$  of 0.33 at 700 K have been reported for Cu<sub>0.97</sub>Fe<sub>1.03</sub>S<sub>2</sub>.<sup>[51]</sup> Also, an enhancement has been found for sulfur deficient chalcopyrite, with  $zT$  0.21 at 573 K reported for CuFeS<sub>1.8</sub><sup>[52]</sup> or when introducing a magnetic cation to substitute part of the copper, with  $zT$  of 0.2 at 673 K for Cu<sub>0.98</sub>Co<sub>0.02</sub>FeS<sub>1.98</sub>.<sup>[53]</sup> Another ternary compound that exhibits low thermal conductivity at its stoichiometric composition is bornite, Cu<sub>5</sub>FeS<sub>4</sub>, where values of  $zT$  of 0.55 at 543 K have been reported for ball-milled samples.<sup>[54]</sup> Out of the stoichiometry, much higher values have been achieved, such as  $zT = 0.6$  at 550 K for variations between copper and iron<sup>[55]</sup> or even  $zT$  of 0.79 at 550 K if the hole concentration is also adjusted. Substitution of iron and copper sites has also been investigated with cobalt ( $zT = 0.5$  at 590 K for Cu<sub>4.96</sub>Co<sub>0.04</sub>FeS<sub>4</sub><sup>[56]</sup>) and cobalt and zinc ( $zT = 0.6$  at 590 K, Cu<sub>4.96</sub>Co<sub>0.04</sub>Fe<sub>0.96</sub>Zn<sub>0.04</sub>S<sub>4</sub><sup>[57]</sup>). The Cu–Sn–S ternary compounds are also promising thermoelectric materials, with a  $zT$  of 0.5 at 759 K for the stoichiometric composition Cu<sub>7</sub>Sn<sub>3</sub>S<sub>10</sub>, which can be increased to values of  $zT$  around 1 at 750 K when doped with Br.<sup>[58]</sup>

Finally, among the copper sulfides, the family of synthetic coulosites (Cu<sub>26</sub>A<sub>2</sub>E<sub>6</sub>S<sub>32</sub>, being A = V, Ta, Cr, Mo, and E = Sn,

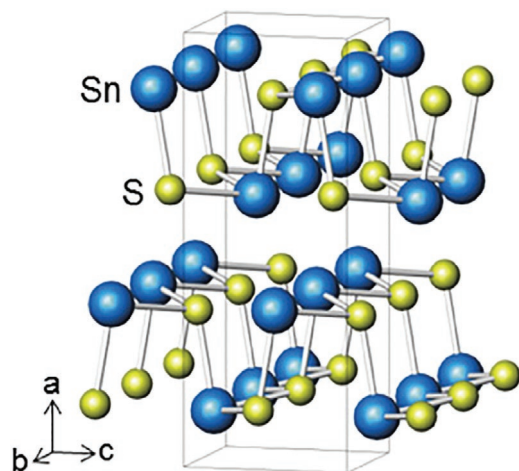


**Figure 4.** Crystal structure of SnS. Reproduced with permission.<sup>[65]</sup> Copyright 2016, The Japan Society of Applied Physics.

As possible earth-abundant components) has emerged recently as a promising source of cost-effective and sustainable thermoelectric materials. A recent thorough review on coulosites by Guélou et al. is available in reference.<sup>[16]</sup> Values of  $zT$  of 0.56 at 663 K has been found for Cu<sub>26</sub>V<sub>2</sub>Sn<sub>6</sub>S<sub>32</sub>,<sup>[59]</sup> 0.78 at 660 K for Cu<sub>26</sub>Ta<sub>2</sub>Sn<sub>6</sub>S<sub>32</sub>,<sup>[60]</sup> and even as high as 0.93 at 675 K for Cu<sub>26</sub>V<sub>2</sub>Sn<sub>6</sub>S<sub>32</sub><sup>[61]</sup> or 0.96 at 670 K for Cu<sub>26</sub>Ta<sub>2</sub>Sn<sub>5.5</sub>S<sub>32</sub>.<sup>[60]</sup>

Within the same group are the orthorhombic compounds of groups IV–VI such as GeS and SnS (see **Figure 4** for its crystalline structure). Thus, first-principles calculations predict Seebeck coefficient values for SnS of ≈668  $\mu\text{V} \cdot \text{K}^{-1}$  at 650 K and very low thermal conductivity values ( $\kappa \approx 0.1 \text{ W} \cdot \text{m}^{-1} \cdot \text{K}^{-1}$ ) leading to figure-of-merit values of  $zT \approx 1$  up to 700 K. Experimental work to date supports those theoretical expectations by demonstrating that polycrystalline Ag-doped SnS exhibits a figure of merit values of ≈0.6 at 873 K<sup>[62]</sup>. More recently, higher values for SnS have been obtained, with a  $zT$  of 0.8 at 873 K.<sup>[63]</sup> The GeS compound was found to have slightly lower thermoelectric properties than SnS.<sup>[64]</sup>

It should be noted that in recent years there has been increasing interest in sulfides with a layered structure. This structure presents thermoelectric advantages. For example, the compounds typically exhibit low thermal conductivity ( $<10 \text{ W} \cdot \text{K}^{-1} \cdot \text{m}^{-1}$ ), allow easy intercalation of atoms between the layers, and show anisotropy in different properties such as thermal conductivity or optical properties. These compounds, therefore, have “a priori” good prospects to be explored as thermoelectric compounds. The best known are those belonging to the disulfide family, such as MoS<sub>2</sub>, WS<sub>2</sub>, and TaS<sub>2</sub>,<sup>[66]</sup> though the reference compound is titanium disulfide (TiS<sub>2</sub>). This sulfide has a value of  $S \approx -170 \mu\text{V} \cdot \text{K}^{-1}$ , the electrical conductivity of  $5.5 \times 10^4 \text{ S} \cdot \text{m}^{-1}$  at 300 K,<sup>[67]</sup> and the thermal conductivity of  $6.8 \text{ W} \cdot \text{m}^{-1} \cdot \text{K}^{-1}$ . So, TiS<sub>2</sub> shows a figure of merit of  $zT \approx 0.16$  at 300 K,<sup>[68]</sup> which makes it a compound of considerable interest for thermoelectric applications, moreover taking into account that nanostructuration is known to reduce the thermal conductivity.<sup>[6]</sup> To reduce the thermal conductivity and improve the electrical properties, different substitutions of Ti with elements that can provide charge transfer to the TiS<sub>2</sub> have been studied. Values of  $zT$  slightly higher than those of TiS<sub>2</sub> were found for Ti<sub>0.95</sub>Ta<sub>0.05</sub>S<sub>2</sub>,<sup>[69]</sup> while an effective reduction

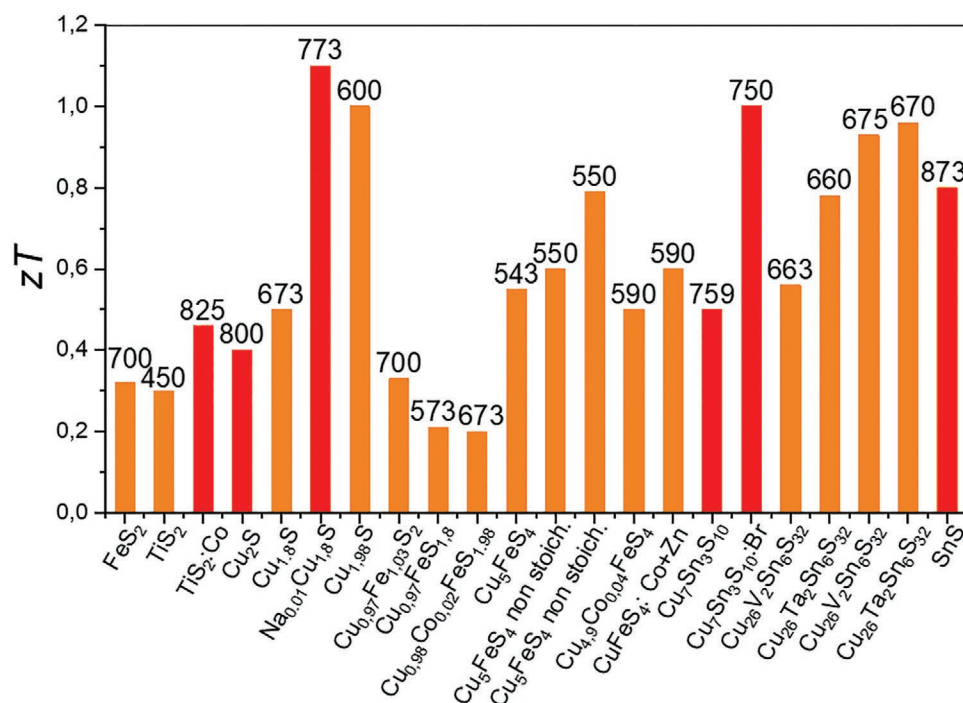


**Figure 5.** Summary of the highest reported  $zT$  values for different sulfide materials. The temperature at which the samples are measured is indicated on the label. Red represents materials with the maximum  $zT$  at temperatures higher than 700 K and orange for medium-range temperatures between 400 to 700 K (data from the documents reviewed in this section and Refs. [51,74–76]).

of the thermal conductivity was obtained when introducing Co, obtaining an n-type material of  $zT = 0.30$  at 573 K.<sup>[70]</sup> The highest value for these compounds, when using earth-abundant dopants, was obtained by copper substitution, with a  $zT$  of 0.46 at 825 K for  $\text{Cu}_{0.1}\text{TiS}_2$ .<sup>[71]</sup> Furthermore, these compounds can be exfoliated, which has become an interesting playing field to study the fundamental and applied thermoelectric properties of 2D compounds as a recent review has shown.<sup>[30]</sup>

In this respect, recent attention has been given to a new family of layered sulfides, the metal trisulfides ( $\text{MS}_3$ ,  $\text{M} = \text{Ti}$ ,  $\text{Zr}$ ,  $\text{Hf}$ ,  $\text{Nb}$ ,  $\text{W}$ ). Work going back over 30 years has shown that they typically have high Seebeck coefficient values ( $500\text{--}800 \mu\text{V}\cdot\text{K}^{-1}$ ) but also moderately low electrical conductivity values ( $1\text{--}100 \text{S}\cdot\text{m}^{-1}$ ). The most investigated is the bulk titanium trisulfide  $\text{TiS}_3$ , which exhibits  $S \approx -625 \mu\text{V}\cdot\text{K}^{-1}$  and  $\sigma \approx 61 \text{S}\cdot\text{m}^{-1}$  at 523 K, with which solid solutions have been made with Niobium in the ratio  $x = 0.1$  allowing to obtain an  $S \approx -340 \mu\text{V}\cdot\text{K}^{-1}$  and  $\sigma \approx 123 \text{S}\cdot\text{m}^{-1}$  at 523 K.<sup>[72]</sup>

Chalcogenide perovskites have recently been considered promising thermoelectric candidates.<sup>[5,73]</sup> These materials have an  $\text{ABX}_3$  crystalline structure and good optical and electronic properties, but they have barely been explored. Perovskite structure allows adjusting the band structure by varying the chemical composition due to the high tolerance of the stoichiometry. Additionally, different defects (A-cation deficient, B-cation deficient, anion deficient) could provide different types of conductivity. For instance, calculations<sup>[36]</sup> have shown that  $zT$  near 1 with ultralow thermal conductivities is  $\text{CaZrSe}_3$  opened new routes for their sulfides counterparts. **Figure 5** summarizes the best-reported  $zT$  values measured in these materials.

Finally, it is remarkable that many sulfides have high values of energy gap (more than 2 eV) which are generally

discarded for thermoelectric applications show interesting photo-thermoelectric properties. For instance,  $\text{ZnS}$  thermopower values could be adjusted under illumination, due to a photoexcited transport carrier effect,<sup>[77]</sup> which could lead to new pathways for these compounds.

Sulfides are synthesized in different ways (see **Figure 6**). The most traditional method is via solid-state techniques with thermal or mechanical energy input. In the first group, the elements are mixed with sulfur and heated at high temperatures ( $>500 \text{ }^\circ\text{C}$ ) for long periods (weeks to even months). Heating is performed in an inert atmosphere to prevent reaction with oxygen, which considerably slows down the reaction. Furthermore, this method is only capable of reaching stable phases, which considerably limits the possibility of synthesizing new compounds. To overcome this problem, other techniques which may produce metastable phases such as milling/mechanical alloying are used.<sup>[78]</sup> In this case, the elements and sulfur are milled by using different mills able to reach different input energies from  $0.01 \text{W g}^{-1}$  ball to  $1 \text{W g}^{-1}$  ball (planetary, Spex). During milling, the material is subjected to different phenomena such as compression, deformation, local heating, etc., resulting from the impact of the balls. Consequently, a nanocrystalline (with a huge amount of grain boundaries), or even an amorphous structure, could be synthesized. Moreover, the high pressures (GPa) to which the material is subjected during the milling process could generate new metastable phases. Both methods are easily scalable and can be implemented in the industry.<sup>[37]</sup> These structures can be made by SPS, a widely used method that contributes to agglomerate the milled powder preventing the crystallite size growth.<sup>[73]</sup>

To synthesize thin films, layered or 2D sulfides, other methods are required. A simple sulfur-solid reaction is an easy

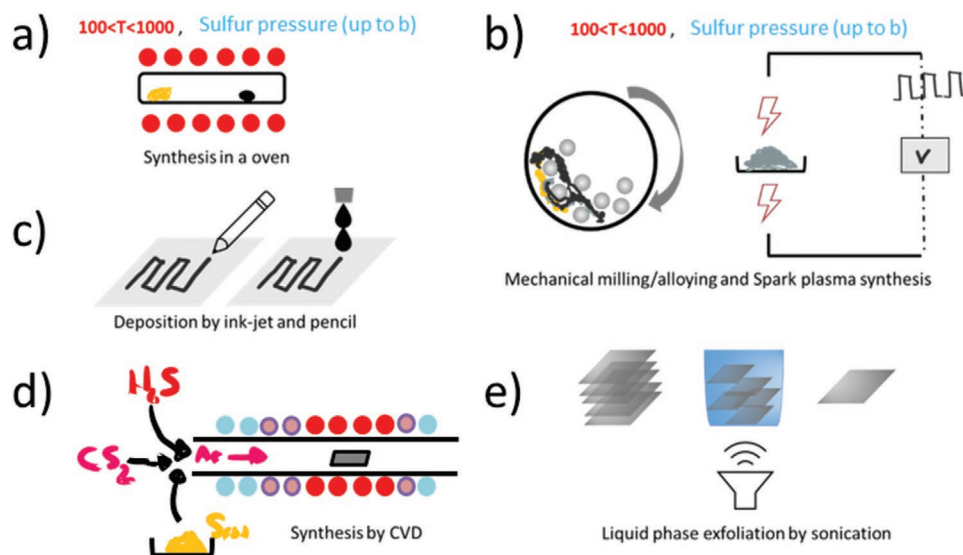


**Figure 6.** Scheme of different sulfide synthesis methods along with the typical temperatures and conditions used: a) Synthesis in a close system, b) mechanical milling and spark plasma synthesis, c) ink-jet or pencil printing methods, d) CVD, and e) liquid-phase exfoliation by sonication.

way of producing films. The gas-film reaction occurs in a sealed ampoule under temperature (RT–1000 °C) and controlled sulfur pressure (up to several atmospheres). Reactive sputtering could also be performed to obtain sulfide films.<sup>[35,65,74]</sup>

Sulfides are often synthesized via chemical vapor deposition (CVD). The technique consists of mixing reacting elements such as metals or compounds such as carbonates and oxides with gas or vapor streams, typically H<sub>2</sub>S, CS<sub>2</sub>, or even sulfur gas. This method has been one of the most promising (and simplest) methods of producing 2D materials of large-area and high-quality,<sup>[79,80,81]</sup> such as GaS, MoS<sub>2</sub>, or WS<sub>2</sub>. Other synthetic methods include mechanical exfoliation, chemically assisted exfoliation, atomic layer deposition, and screen printing deposition.<sup>[51,75,82]</sup>

Due to the low figure of merit, most of the applications that have been developed based on sulfides are placed on preliminary prototypes.<sup>[76,83]</sup> Moreover, many of them have low melting points which improve different phenomena such as sulfur diffusion, phase segregation, or even decomposition. These circumstances should promote low-temperature applications in this family of compounds.

### 3. Tetrahedrites

Tetrahedrites were originally named due to their tetrahedral morphology in 1845.<sup>[84]</sup> Nowadays, tetrahedrite minerals are the major source of Cu, Sb, and S. Tetrahedrites (along with tennantite, Cu<sub>12</sub>As<sub>4</sub>S<sub>13</sub>, which crystallize into an isomorphous cubic structure) have a rather high thermoelectric performance.<sup>[85]</sup> Although tetrahedrites have been known as minerals for a long time, they were identified as good thermoelectric materials around 2012.<sup>[84]</sup> In the case of synthetic stoichiometric tetrahedrites, *zT* values around 0.6 for 723 K have been reported.<sup>[86,87]</sup> With the highest reported value of 0.76 at 623 K.<sup>[88]</sup> Even though they contain Sb, which is quite scarce on the earth-crust, being the tetrahedrite composition Cu<sub>12</sub>Sb<sub>4</sub>S<sub>13</sub>, Sb represents 30% of the weight, and it is usually considered an environmentally

friendly compound.<sup>[15]</sup> Out of the stoichiometry, there have been studies on copper-rich tetrahedrites, which show a mixture of two different phases, with the excess of copper reducing the thermal conductivity and showing a phonon liquid electron crystal behavior.<sup>[89]</sup>

The tetrahedrites are a particularly important type of natural minerals. They have the general chemical formula of A<sub>10</sub>B<sub>2</sub>X<sub>4</sub>Y<sub>13</sub>, being A either Cu or Ag, B a transition metal (for instance, Ni, Fe, Zn, Mn, Co or Hg), X either Sb or As (and sometimes Bi or Te) and finally, Y is S, that can be partially substituted by Se.<sup>[90]</sup> It has a complex crystallographic structure, being the Cu<sub>12</sub>Sb<sub>4</sub>S<sub>13</sub> a body-centered cubic structure, sometimes described as a complex defective sphalerite structure, with the transition-metal cations localized in tetrahedral and trigonal planar sites and the pnictogen atoms in trigonal-pyramidal sites (see **Figure 7**).<sup>[89,91]</sup> Tetrahedrites are based on earth-abundant, non-toxic, and non-expensive elements. These characteristics are essential for the development of large-scale applications. Natural occurring tetrahedrite (Cu<sub>10</sub>Zn<sub>2</sub>As<sub>4</sub>S<sub>13</sub>)

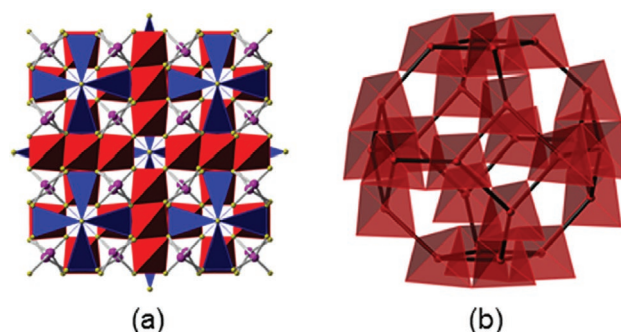


**Figure 7.** Crystal structure of Cu<sub>12</sub>Sb<sub>4</sub>S<sub>13</sub> tetrahedrite a) along [100] with the CuS<sub>4</sub> tetrahedra in red and the CuS<sub>3</sub> trigonal units in blue, b) the sodalite cage created by the linkage of the CuS<sub>4</sub> tetrahedra. In both cases, the Cu(1) and Cu(2) atoms are indicated in red, S, in yellow, and Sb atoms in magenta. Reproduced with permission.<sup>[15]</sup> Copyright 2019, American Institute of Physics.

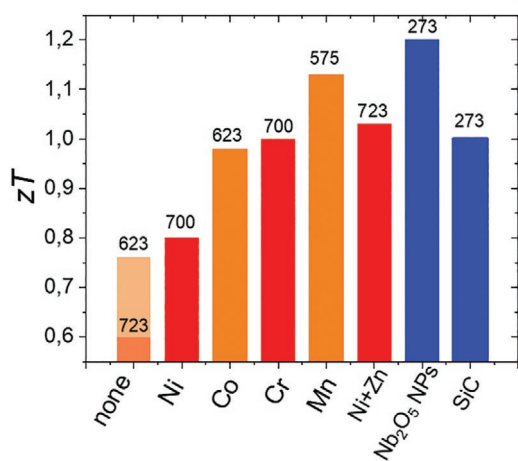


**Figure 8.** Summary of the highest reported  $ZT$  values for different tetrahedrites. The maximum  $ZT$  temperature is shown in the label (around room temperature in blue, over 400 K in orange, and over 700 K in red). The different tetrahedrites are those without dopants (stoichiometric composition), with different earth-abundant dopants (Ni, Co, Cr, Mn, and co-doping of Ni and Zn), and when Nb<sub>2</sub>O<sub>5</sub> nanoparticles or SiC are used. The references to these values are given in this section.

and the synthetic Cu<sub>12</sub>Sb<sub>4</sub>S<sub>13</sub> are p-type thermoelectric materials that have a degenerate semiconducting electronic structure, with the Fermi level lying in the valence band<sup>[92,93]</sup> and a pseudo-gap of around 1.2 eV.<sup>[86]</sup> Tetrahedrites are attractive for thermoelectric applications because they have a very low intrinsic thermal conductivity, which is sometimes related to the large anharmonic vibrations of the Cu(2) atoms in the structure, which act as rattlers.<sup>[89]</sup>

Tetrahedrites have attracted much attention lately from the thermoelectric community, and therefore, reviews discussing this material can be found in the literature.<sup>[15,47,84,94]</sup> In this work, we will concentrate on the latest developments in their thermoelectric properties. The most usual way of improving the thermoelectric performance of tetrahedrites has been the substitution of transition elements in Cu, generating materials with the formula Cu<sub>12-x</sub>M<sub>x</sub>Sb<sub>4</sub>S<sub>13</sub>, where M can be earth-abundant cations such as Cr, Mn, Fe, Co, Ni, Cu, Zn, or the element Mg<sup>[15,92]</sup> (see **Figure 8**). Results of Ni substitution showed an increased Seebeck coefficient and reduced thermal conductivity, with an improved  $zT$  value of 0.8 at 700 K for Cu<sub>10.4</sub>Ni<sub>1.6</sub>Sb<sub>4</sub>S<sub>13</sub> in the case of solid-state fabrication methods,<sup>[87]</sup> and a little lower in the case of mechanical alloying preparation.<sup>[95]</sup> In a similar study, Heo et al. found that the highest power factor is that of the un-substituted tetrahedrite, Cu<sub>12</sub>Sb<sub>4</sub>S<sub>13</sub>, while the ones with certain substitution presented reduced thermal conductivity.<sup>[96]</sup> The highest measured  $zT$  values for tetrahedrites doped with earth-abundant elements have been those reported for Cu<sub>11.5</sub>Co<sub>0.5</sub>Sb<sub>4</sub>S<sub>13</sub>, with  $zT$  of 0.98 at 623 K<sup>[97]</sup>, Cu<sub>11.65</sub>Cr<sub>0.35</sub>Sb<sub>4</sub>S<sub>13</sub>, with  $zT$  of 1.0 at 700 K,<sup>[98]</sup> Cu<sub>11</sub>MnSb<sub>4</sub>S<sub>13</sub>, with  $zT$  of 1.13 at 575 K.<sup>[96]</sup> Co-doping with Ni and Zn was also tried,<sup>[99]</sup> obtaining a 30% increase in the  $zT$  of Cu<sub>10.5</sub>NiZnSb<sub>4</sub>S<sub>13</sub>, which reached values of 1.03 at 723 K. It is worth saying that the  $zT$  values obtained when the doping was performed with rare earth elements have only reached those listed here, but not exceeded them, with a maximum reported value of  $zT$  of 0.92 at 723 K for Te doping.<sup>[15,100]</sup>

To further increase the thermoelectric properties of the tetrahedrites, different studies have been carried out by introducing dopant atoms at Sb<sup>[90]</sup> or S<sup>[101]</sup> sites, obtaining a reduction in the thermal conductivity when introducing Te due to a certain phase separation in the first case, and Bi in the second case.

Furthermore, the approximation of improving the thermoelectric performance by nanostructuring has also been studied in the case of tetrahedrites. A work by Sun et al. in 2019 showed a fine-grained nanostructured composite based on tetrahedrites with Nb<sub>2</sub>O<sub>5</sub> nanoparticles dispersed on it.<sup>[102]</sup> In this way, the thermal conductivity was reduced and a  $zT$  as high as 1.2 at 273 K was achieved. More recently, in 2020, the combination of modified tetrahedrite nanoparticle composites, showed reduced thermal conductivity maintaining a relatively high electrical conductivity, achieving values of  $zT$  of 1 at 273 K when a small quantity of SiC was introduced.<sup>[103]</sup>

Even though tetrahedrites have been known for a long time, some of their properties are not fully understood. Indeed, in 2020 the low-temperature structure, that is, the stable one below its metal-to-semiconductor transition, was studied for the first time.<sup>[104]</sup> This is an example of how there is still room for research in understanding the physical relations between phonon transport, crystal structure, and electronic properties, which are necessary to improve their thermoelectric performance.

Given the fact that metal sulfides are difficult to synthesize due to the volatility of sulfur and its easiness to oxidize, the most used synthesis methods require a sealed tube or solvothermal conditions under an inert atmosphere. Therefore, the most common method for producing synthetic tetrahedrites is by solid-state reactions under a controlled atmosphere, usually in a glovebox filled with argon. The starting materials or precursors are placed in quartz tubes and sealed under vacuum, and then the ampoules are heated at temperatures over 700 K for a certain time (even days) and then quenched down (see for instance<sup>[90]</sup>) or cooled down, then grounded and then annealed again.<sup>[89]</sup> In other cases, subsequent annealing periods at different temperatures are performed, and the single crystals are selected from the obtained ingots.<sup>[85]</sup> In some cases, the obtained ingots are then grounded and hot-pressed under vacuum.<sup>[96,101,105]</sup> Another method used is the solvothermal method, but it requires expensive solvents and leads to long processes with low yields.<sup>[95]</sup>

In the case of nanocomposites based on tetrahedrites, the fabrication method combined mechanical alloying and SPS.<sup>[102,103]</sup> It is also possible to obtain large amounts of pure and non-toxic tetrahedrite compound by high-energy mechanical alloying from the elemental precursors, as presented by Barbier et al.<sup>[106]</sup> In this case, the pure powdered elements were stoichiometrically mixed and placed in tungsten carbide jars containing tungsten carbide balls, and then high-energy ball-milled under controlled atmosphere (argon) and also in air. Then, the resulting powder was compacted using SPS. Or, in other cases, the mechanical alloying of the elements can be hot-pressed.<sup>[107]</sup>

Synthetic tetrahedrites for thermoelectric applications can be also obtained in great quantities if previously synthesized material is mixed with the natural mineral tetrahedrite, as it was presented in the work of Lu et al.<sup>[108]</sup> In this work, they pulverized synthetic tetrahedrites to powder with a mortar and pestle,



and then, these powders were mixed with natural mineral powders and milled together with stainless steel balls. Different proportions of synthetic and natural tetrahedrites were then charged onto a vial and sealed in a glove box filled with argon and milled for 30 min. The fine powder was then loaded into a graphite die and hot pressed in an argon atmosphere. This manufacturing method reduces the cost by using the natural mineral as a source, which is highly abundant in the Earth's crust, with  $zT$  obtained up to 1 at 700 K.

Tetrahedrites, which have a maximum thermoelectric efficiency conversion for applications at temperatures around 700 K, can be used in industrial heat recovery, for instance. There was a company, Alphabet Energy, which took advantage of the naturally occurring tetrahedrites and used them as p-type material in their modules (the n-type material used was magnesium silicide).<sup>[109]</sup> The company operated from 2009 to 2018 and developed industrial-scale thermoelectric generators that converted heat from the exhaust gases from large industrial engines. It was capable of producing up to 25 kWe from a 1000 W motor.

Anyway, the development of devices based on tetrahedrites, thermal stability, mechanical properties, thermal barriers, contact resistances, etc. demands an additional investigation. Besides, a compatible n-type material should also be found and the appropriate contact resistances optimized.

#### 4. Earth-Abundant Oxides

Oxide-based materials are used in a wide variety of applications at high temperatures, such as energy generation, conversion, or storage (solar cells, fuel cells, nuclear reactors, batteries, catalytic converters, etc.).<sup>[110]</sup> They are generally inexpensive and easy to prepare, and they overcome some problems with metal-based materials at high temperatures, such as their tendency to corrosion, thereby reducing their electrical conductivity. Different transition metal oxides can be used for different temperature ranges, from cryogenics to high temperatures. Some of the elements which are abundant in the earth's crust and industrially produced in large numbers such as Ti, Mn, Cu, Zn, Mo, or W, form oxides that have interesting thermoelectric properties, as other abundant and non-toxic elements, such as V and Co (see Figure 1). As a result of their extensive use in different technologies, it is known how to adjust their electronic properties by doping, stoichiometric control, or morphological changes. However, their presence in the thermoelectric arena is relatively new, and it was triggered by the work of Terasaki et al. in 1997 on  $\text{NaCo}_2\text{O}_2$ .<sup>[111]</sup> In principle, oxides have quite high thermal conductivities, which is the main reason why they have not been taken into account for thermoelectrics application until  $\text{NaCo}_2\text{O}_4$  was presented as a promising material. Apart from these narrow bandgap semiconductors that can be grouped under the denomination of non-stoichiometric cobalt oxides (or layered cobaltites) composed of earth-abundant elements, such as  $\text{Na}_x\text{CoO}_2$  and  $\text{Ca}_3\text{Co}_4\text{O}_9$ , there is also another family of wide bandgap semiconductors, those formed by the transition metal oxides, which have shown promising thermoelectric properties.

Starting with the element with the lower atomic number of the above-cited transition metal oxides, Ti, its oxide, that

is,  $\text{TiO}_2$  is a widely investigated material for its applications in photocatalysis, biosensing, solar cells, etc. It exhibits a bandgap around 3.2 eV and it presents many polymorphs, of which anatase, brookite (orthorhombic), and rutile (tetragonal) are the most common. At room temperature, anatase is the dominant polymorph, turning into brookite and then rutile at high temperatures (over 1275 K).

The next one would be manganese oxide, which has a smaller bandgap of about 1.3 eV and is used in electrochemical batteries, electrodes for supercapacitors, etc. It has different polymorphs, like  $\alpha\text{-MnO}_2$  psilomelane, with monoclinic structure and  $\beta\text{-MnO}_2$ , with pyrolusite-rutile structure (see for instance Ref. [112]).

Copper presents two phases which occur quite commonly in nature: cuprous oxide or cuprite  $\text{Cu}_2\text{O}$  (indirect bandgap around 1.9 to 2.2 eV), with applications in catalysis, sensing and solar cells, and cupric oxide or tenorite,  $\text{CuO}$  (direct bandgap around 1.2 to 1.5 eV), with is the basis for different high-temperature superconductors. The first has a cubic crystalline structure while the second has a monoclinic crystalline structure, which is almost an electrical insulator in its stoichiometric composition.

From the family of metal oxides, it can be said that  $\text{ZnO}$  is the most studied because it has applications in photovoltaic, optoelectronic, piezoelectric, detection, and thermoelectricity.<sup>[113]</sup> It has a direct band-gap of about 3.3 eV and can have several structures, such as cubic zinc-blende, wurtzite (which is the stable polymorph at room temperature).

Molybdenum oxides are present in different stoichiometries, being  $\text{MoO}_3$  the most widely reported, with an indirect bandgap of 3 eV and an orthorhombic structure, with a more stable phase, the  $\alpha\text{-MoO}_3$  layered structure which is reached at temperatures above 620 K. In the case of tungsten oxides, the most commonly reported is  $\text{WO}_3$ , which is an n-type material with a perovskite-like structure, with a bandgap between 2.6 and 3.25 eV,<sup>[114]</sup> and it is usually found in its hydrated form  $\gamma\text{H}_2\text{O}\cdot\text{WO}_3$ . In the case of vanadium, from its different oxides, only  $\text{V}_2\text{O}_5$ , which has an orthorhombic structure,<sup>[115]</sup> has promising thermoelectric properties. This is an n-type semiconductor with a direct bandgap of about 2.4 eV, which has been used as an electrode in energy storage systems and has a layered structure.

Finally, cobalt oxide is also widely studied due to its different applications in catalysis, energy storage, detection, and so on. There are two main stable forms of cobalt oxide:  $\text{Co}_3\text{O}_4$ , which exhibits a cubic lattice, it is a spinel with both  $\text{Co}^{2+}$  and  $\text{Co}^{3+}$  and with a bandgap between 1.4 and 1.8 eV;  $\text{CoO}$  also has a cubic structure, with a bandgap between 2.2 and 2.8 eV. Both are usually found in excess oxygen compositions, resulting in p-type semiconductors.

Transition metal oxides and their applications as thermoelectric materials have been the focus of different studies and reviews.<sup>[116–121]</sup> As it has been said, in this work, we will focus only on those based on earth-abundant elements, but even with this requirement, there are many possible oxides with interesting thermoelectric properties.

In the case of  $\text{TiO}_2$ , its non-stoichiometric form showed promising thermoelectric properties for different application ranges. In 2006, values up to  $S = -518 \mu\text{V}\cdot\text{K}^{-1}$  and

$\sigma = 2 \times 10^3 \text{ S} \cdot \text{m}^{-1}$  at 350 K were reported for  $\text{TiO}_{1.94}$ .<sup>[122]</sup> A few years later, in 2009, exceptional properties at cryogenic temperatures were found, with a  $zT$  of 0.1 at 10 K.<sup>[123]</sup> Another way of improving the thermoelectric properties is to use dopants, such as Na, along with nanostructuring, fabricating nanotubes, obtaining  $zT$  values up to 0.3 at 745–1032 K.<sup>[124]</sup>

Manganese oxide is an n-type material. The most well-known stoichiometry for thermoelectric applications is that of  $\text{CaMnO}_3$ , with  $zT$  values of 0.15 for 1173 K.<sup>[125]</sup> This value can be improved by doping with different rare-earth elements. Nevertheless, in the same work of Thiel et al., they reported tungsten doping, obtaining a  $zT$  value of 0.25 at 1223 K.<sup>[125]</sup>

Cuprous oxide,  $\text{Cu}_2\text{O}$ , has a Seebeck coefficient as high as  $1050 \mu\text{V} \cdot \text{K}^{-1}$  at temperatures of 923 K.<sup>[126]</sup> In the form of thin-films, with both the copper oxides mixed in it, Seebeck values up to  $204 \mu\text{V} \cdot \text{K}^{-1}$  were reported, along with an electrical conductivity of  $50 \text{ S} \cdot \text{m}^{-1}$  at room temperature,<sup>[127]</sup> but the thermal conductivity does not appear reported in those works, so in this case, there is still room for studying the material for thermoelectric applications.

Zinc oxide can be synthesized in a wide variety of morphologies, such as bulk ceramics,<sup>[128]</sup> thin films,<sup>[129,130]</sup> and a wide variety of nanostructures.<sup>[18]</sup> At room temperature, ZnO shows a power factor,  $S^2 \cdot \sigma$  quite high, of around  $800 \mu\text{W} \cdot \text{m}^{-1} \cdot \text{K}^{-2}$ , but the thermal conductivity exhibited is also high, of around  $40 \text{ W} \cdot \text{m}^{-1} \cdot \text{K}^{-1}$ , which is reduced for increasing temperatures, reaching  $5 \text{ W} \cdot \text{m}^{-1} \cdot \text{K}^{-1}$  at 100 K.<sup>[131]</sup> A means of reducing the thermal conductivity that has been widely used in the case of ZnO, as it will be discussed later for metal oxides, is through nanostructuring. Nevertheless, an important improvement of the thermoelectric properties can also be obtained through doping, for instance with Al,<sup>[132–134]</sup> Ge,<sup>[135]</sup> Ni,<sup>[136]</sup> Ga,<sup>[137]</sup> or Ti (all of them, earth-abundant elements). The best results, as far as thermoelectric efficiency is concerned, have been obtained when co-doping has been done, obtaining for a composition of  $\text{Zn}_{0.96}\text{Al}_{0.03}\text{Ga}_{0.02}\text{O}$   $zT$  values of 0.45 and 0.65 at 1000 and 1247 K, respectively.<sup>[138]</sup>

Molybdenum oxides, both doped and non-stoichiometric, showed high power factors, but low figures of merit, such as that reported for  $\text{Mo}_{17}\text{O}_{47}$  of 0.039 at 690 K.<sup>[139]</sup> The best thermoelectric properties to date for molybdenum oxides have been found when rare-earth elements were used for doping, to introduce heavy transition metals, which is out of the scope of this review, due to their scarcity on the earth-crust according to Figure 1.

Tungsten oxide is also n-type, and there is little work dealing with its thermoelectric performance. Non-stoichiometric tungsten oxide, prepared by SPS, showed moderate thermoelectrical properties, with a maximum  $zT = 0.061$  for  $\text{WO}_{2.90}$  at 963 K.<sup>[140]</sup> Something similar is happening with vanadium, where low values for relevant thermoelectric applications have also been reported for vanadium oxide, without relevant results for this material so far.<sup>[141]</sup>

Finally, non-stoichiometric cobalt oxides are among the metal oxides with the highest  $zT$  values have been reported. Some have layered structures, such as  $\text{Na}_x\text{CoO}_2$ ,<sup>[111,142]</sup> or  $\text{Ca}_3\text{Co}_4\text{O}_9$ .<sup>[143]</sup>  $\text{NaCo}_2\text{O}_4$  has been studied for thermoelectric applications, with a reported  $zT$  of 0.05 at room temperature,<sup>[144]</sup> but it has the drawback of the volatility of Na and its degradation above

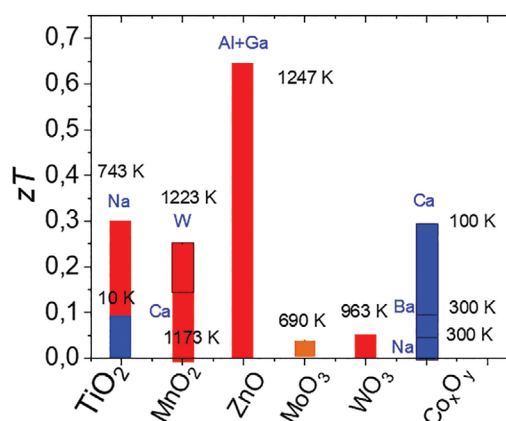


**Figure 9.** Summary of the highest reported  $zT$  values for the different earth-abundant oxides, with the temperature at which they are measured added on the label (room temperature and lower, blue, 400–700 K orange, and over 700 K, red). The metal that forms the oxide is shown in the x-axis, and when different earth-abundant elements are introduced into their structure, these are shown with a blue label. References are included in Section 4.

1173 K. Ba has resulted in a better dopant, with reported  $zT$  values at room temperature of 0.11 for layered  $\text{Ba}_{0.27}\text{CoO}$  composition,<sup>[145]</sup> or Ca, with a  $zT$  of around 0.3 at 100 K for the composition  $\text{Ca}_3\text{Co}_4\text{O}_9$ .<sup>[146]</sup> Moreover, measurements in single crystals of  $\text{Ca}_3\text{Co}_4\text{O}_9$  have reported values of  $zT$  of 0.87 at 973 K.<sup>[142]</sup> Further improvements of cobalt oxides rely on the addition of precious metals or rare earth as dopants (such as Ag, Gd, La, etc.), which will not be discussed in this review for their scarcity. Also, 2D confined systems such as whiskers of single crystals of  $\text{Ca}_3\text{Co}_4\text{O}_9$  have been estimated to have  $zT$  values of 1.7 to 2.7 at 873 K (taking the thermal conductivity of a polycrystalline sample).<sup>[147]</sup> These predictions have encouraged the research of 2D configurations with these kinds of layered oxides, in which the confinement in one direction can give rise to a reduction of the thermal conductivity due to enhanced phonon scattering and also quantum effects that enhance the electrical properties. **Figure 9** summarizes the best-reported  $zT$  values for the different earth-abundant oxides described in this section.

One way of engineering the transition metal oxides for obtaining higher thermoelectric performance is through substructuring (or segmentation), which is a route to decouple the lattice and electronic contributions to the thermal conductivity. It consists of a periodic arrangement of layers of different characteristics, as far as electron and phonon transport is concerned. This results in complex material structures, that ideally include a high mobility material along with a phonon scattering material.<sup>[148]</sup> Some transition metal oxides may be found as superlattices in their natural state, such as doped cobalt oxide.<sup>[111]</sup>

Another way to increase the thermoelectric performance of the above-mentioned metal oxides is by nanostructuring,<sup>[121]</sup> as was done for  $\text{TiO}_2$ ,<sup>[124]</sup> manganates,  $\text{ZnO}$ ,<sup>[149]</sup> or cobalates. A review of the effects of nanostructuring in different oxides can be found in reference.<sup>[17]</sup> With the fabrication of nanostructures of these materials, the phonon scattering in the surfaces is enhanced while the electrical transport is for the most part unchanged. Other transition metal oxides, such as iron oxides (which exhibit interesting power factors, as reported

in<sup>[150]</sup>) could be also target materials for thermoelectric applications if their thermal conductivity could be reduced via nanostructuring.

Several different methods can produce metallic oxides. The most commonly used are vapor chemical-based techniques, but also chemical synthesis such as sol-gel hydrolysis, solvothermal<sup>[151]</sup> or electrochemical methods,<sup>[113]</sup> such as Ti anodization, and hydrothermal synthesis are widely used for producing different oxides. Vapor deposition techniques such as atomic layer deposition,<sup>[152]</sup> sputtering,<sup>[127]</sup> molecular beam epitaxy,<sup>[153]</sup> or pulsed laser deposition<sup>[133,154]</sup> can also be used to form highly crystalline oxides. Finally, sintering methods such as SPS<sup>[140]</sup> or solid-state reactions<sup>[138]</sup> have also been used to form certain metal oxides

There is one manufacturer that uses calcium and manganese oxides as thermoelectric materials in their modules: TECTEG.<sup>[155]</sup> This company produces modules working up to 800 °C, claiming high stability and durability for up to 50 years with little or no degradation. If the cold side is maintained at 50 °C, the modules with 32 couples should deliver 12.3 W. The price for this module (CMO-32-62S) is 375 \$ in 2021, which is above what would be expected if production were substantial.<sup>[109]</sup> With these modules, studies such as the performance of a system for harvesting thermoelectric energy from asphalt pavement were presented in 2019,<sup>[32]</sup> concluding that the conversion efficiency of the thermoelectric generators should be further improved to optimize the performance of such a harvesting system.

Thermoelectric materials, such as nanocrystalline ZnO, grown in large area cotton fabrics have also been proposed as low-cost flexible thermoelectric power generators.<sup>[151]</sup>

## 5. Silicides

The research on metal silicides as thermoelectrics was started in 1958 by Nikitin.<sup>[156]</sup> Mg<sub>2</sub>Si attracted initially important research attention due to their easy preparation by a solid-state reaction between silicon and the metal<sup>[157,158,159]</sup> and the possibility to tailor its thermal properties and electronic structure by the formation of a solid solution with the general formula (Mg,Ca)<sub>2</sub>(Si,Ge,Sn). Values of *zT* of 0.8 were reported by Marchuck et al.<sup>[160]</sup> in 1989. The Mg<sub>2</sub>Si remains stable until 850 K.<sup>[83]</sup>

Silicide-based thermoelectrics are one of the most promising alloys for the medium temperature (ranging from 500 to 800 K) for power generation, because of their reliable physicochemical properties. Silicon is cost-effective and environmentally sustainable. Among the silicides, Mg<sub>2</sub>Si based (n-type) and higher manganese silicides (HMS) (as p-type) are the most studied materials.

As for the n-type, Mg<sub>2</sub>Si as grown usually forms black colored crystals, with a Fluorite structure with a cubic Fm-3m space. Mg<sup>2+</sup> is bonded to four equivalent Si<sup>4-</sup> atoms to form a mixture of edge and corner-sharing MgSi<sub>4</sub> tetrahedra. All the Mg–Si bond lengths are 2.76 Å. Si<sup>4-</sup> is bonded in a body-centered cubic geometry to eight equivalent Mg<sup>2+</sup> atoms, as shown in **Figure 10**.

Regarding the p-type, known as higher manganese silicide (HMS) or MnSi<sub>x</sub> (with 1.71 ≤ *x* ≤ 1.75) crystals are made

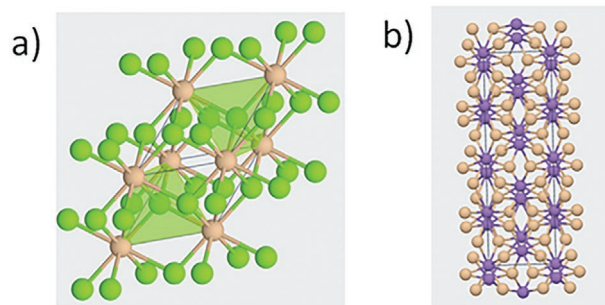


**Figure 10.** Crystal structure of a) Mg<sub>2</sub>Si, showing the Mg (green) and of Si (orange); and b) the incommensurable MnSi<sub>1.75</sub> also known as Mn<sub>4</sub>Si<sub>7</sub> phase showing the Mn (purple) and of Si (orange).

of compositionally homogeneous regions separated by layers of MnSi, oriented along the *c*-axis. They present a complex chimney-ladder crystal structure of tetragonal cells.<sup>[161]</sup> One of the main advantages of these HMS compounds is that they can be obtained with many different compositions, while one of their main drawbacks is the difficulty of synthesizing them as a single phase. They typically have MnSi or Si precipitations as secondary phases, which generally lead to a significant decrease in the power factor and/or increased in  $\kappa$ . Initial investigations on HMS reported *zT* values of 0.3 at 673 K.<sup>[162]</sup> The stability of HMSs depends on the metal ion/s present in the silicide and they can be stable up to 950 K.<sup>[83]</sup>

The performance of n- and p-type silicides has evolved concurrently. A noticeable improvement in the efficiency of Mg<sub>2</sub>Si was achieved in 2011 by Fedorov et al.<sup>[163]</sup> by partially substituting Si for Sn. The Mg<sub>2</sub>Si–Mg<sub>2</sub>Sn solid solutions have been obtained with a *zT* value as high as 1.2 at 750 K. Ternary Mg<sub>2</sub>Si–Si<sub>0.88</sub>Ge<sub>0.12</sub> and FeSi<sub>2</sub>–Si<sub>0.88</sub>Ge<sub>0.12</sub> systems were also proposed in 2009. In these materials, silicides form nano-inclusions that reduce  $\kappa$  by a factor ranging between 4 to 8, thus improving the *zT*.<sup>[164]</sup>

To achieve similar results for the p-type HMS, additional efforts were made due to their complex structure and the complex phase diagram.<sup>[165–167]</sup> Adding or generating inclusions is one of the strategies to enhance the performance of these complex compounds. These inclusions have served as a means of reducing thermal conductivity, as they are centers for phonon scattering. The efforts in obtaining nanocomposites led to an improvement in the HMS efficiency in 2009 when Itoh and Yamada reported that MnSi<sub>1.73</sub> mechanically alloyed with MnSi and then submitted to SPS presented a *zT* of 0.47 at 873 K.<sup>[168]</sup> Within a year, Zhou et al.<sup>[169,170]</sup> found that addition of SiGe to polycrystalline HMS resulted in partial substitution of Ge in Si sites together with the precipitation of SiGe, generating a reduction of  $\kappa_{ph}$  down to 1.6 W m<sup>-1</sup>·K<sup>-1</sup> at 450 °C, without modifying the initial power factor. As a result, a *zT* of 0.5 at 823 K was achieved in the MnSi<sub>1.733</sub>–SiGe composite. The use of nanoprecipitates has also been reported by Luo et al.<sup>[158]</sup> in p-type HMS by obtaining MnSi nano-inclusions. The energy filtering led to an increase of 30% in the electrical conductivity, without modifying the Seebeck, and to a reduction in the thermal conductivity of almost 3 times (from 3.0 to 1.3 W·m<sup>-1</sup>·K<sup>-1</sup>). Because of that, a *zT* of 0.62 at 800 K was achieved. In addition to the generation of nanoprecipitates to boost the *zT*, in 2011 Luo et al.

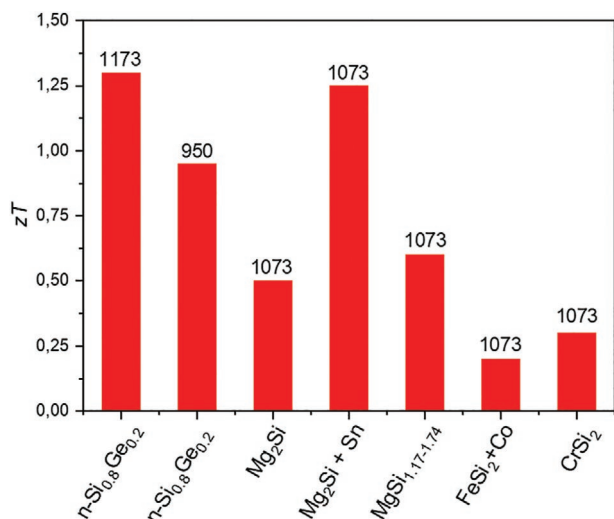


**Figure 11.** Summary of the highest reported  $zT$  values reported for different silicides. The temperature at which the maximum  $zT$  is reached is indicated by the label. Some of the data has been extracted from Ref. [83] or available in the text of this section.

reported a  $zT$  of 0.65 at 850 K by substituting Si by Al in obtaining the phase  $\text{Mn}(\text{Al}_{0.0015}\text{Si}_{0.9985})_{1.80}$ .<sup>[171]</sup>

In 2012, with the help of theory, the increase of  $\text{Mg}_2\text{Si}$  by doping was studied.<sup>[172]</sup> The doping with Al (2.0% mol) gave a  $zT$  up to 0.47 at 823 K.<sup>[173]</sup> While Sb doping with 1.5% mol was shown to increase the  $zT$  up to 0.46 at 810 K.<sup>[174]</sup> Battiston et al.<sup>[175]</sup> reported in 2013 a  $zT$  of 0.50 at 873 K for the 1.0% mol Al-doped in  $\text{Mg}_2\text{Si}$ . In the same year, a  $zT$  of 1.4 at 800 K was reported for Bi-doped and of  $zT = 1.2$  for Sb-doped.

In the more recent years, SiGe inclusions in  $\text{Mg}_2\text{Si}$  have been studied yielding a  $zT$  of 1.3 at 1250 K for  $\text{Si}_{0.88}\text{Ge}_{0.12}\text{-Mg}_2\text{Si}$  nanocomposites.<sup>[176]</sup> In 2014, Gelstein et al. described nanostructured  $n$ -type  $\text{Mg}_2\text{Si}_{1-x}\text{Sn}_x$  and  $p$ -type HMSs with a maximum  $zT$  of 1.1 and 0.6 at 723 K, respectively.<sup>[177]</sup> And, the effect of the addition of nanowires to the HMS has been also tested in 2017. Where tellurium nanowires were embedded in HMS with an increase of  $zT$  from 0.41 to 0.70 at 800 K.<sup>[178]</sup> **Figure 11** summarizes the best-reported values of  $zT$  in silicide.

Other studies that are of importance in the field are the studies on the critical mechanical stability of the silicides.<sup>[179]</sup> Although powders of  $\text{Mg}_2\text{Si}$  may react with water and moisture if they are not encapsulated, it was found that the reaction does not drive crack growth. This is beneficial for the production of devices based on  $\text{Mg}_2\text{Si}$  because the microcracks induced during the operation of the device will not lead to the failure of the thermoelectric generator.

The synthesis of silicide materials can be done by a wide variety of methods, such as induction melting,<sup>[180]</sup> arc melting,<sup>[181]</sup> mechanical alloying,<sup>[182]</sup> solid-state techniques,<sup>[183]</sup> microwave,<sup>[184]</sup> vertical Bridgman growth,<sup>[185]</sup> etc. In most cases, the samples obtained are then grounded and then densified by methods such as hot pressing or SPS.<sup>[186]</sup> In this work, yields of 1 kg per batch were reported for this type of material.

To conclude this section, the most efficient thermoelectric silicides up to date are based on the solid solution  $\text{Mg}_2$  (Si-Sn)

with a  $zT$  of  $\approx 1.5$ <sup>[187–189]</sup> for the  $n$ -type and  $\text{MnSi}_{1.75}$ <sup>[190,191]</sup> or  $\text{ReSi}_{1.75}$ <sup>[192–194]</sup> both with a  $zT$  of  $\approx 0.7$  for the  $p$ -type.

## 6. HH Intermetallic Compounds

Heusler compounds, with the formula  $X_2YZ$ , were first reported by Fritz Heusler in 1903,<sup>[7]</sup> and they have shown great importance, due to their magnetic properties, in the field of spintronics. HH materials are modified Heusler compounds, with the formula  $XYZ$ , that is, with vacancies on the X site. In this review, we will be limited only to the earth-abundant elements, and the HH materials present a wide variety of compositions that meet this requirement.

The first studies as far as thermoelectric properties were concerned were done in HH based on  $\text{MNiSn}$ , being  $M = \text{Ti}$ ,  $\text{Zr}$ , or  $\text{Hf}$ . They showed a high Seebeck coefficient but also high thermal conductivity, so Ni doping was used to reduce it, without reducing their power factor, with a  $zT$  of 0.9 at 960 K for  $\text{Hf}_{0.5}\text{Zr}_{0.25}\text{NiSn}_{0.95}\text{Sb}_{0.025}$ , which was increased to  $zT$  of 1.5 at 700 K for a HH consisting of  $\text{Hf}_{0.5}\text{Zr}_{0.25}\text{NiSn}_{0.95}\text{Sb}_{0.025}$ .<sup>[195]</sup> However, these values have not been reproduced since their publication in 2005.<sup>[7]</sup> Other interesting approaches are those obtained when doping by tin, where a  $zT$  of 0.45 was obtained for  $\text{ZrCoSb}_{0.9}\text{Sn}_{0.1}$  at 958 K,<sup>[196]</sup> excluding the results obtained by introducing Ti or Pd.

In the case of HH compounds based on  $\text{RFeSb}$ , where R stands for V or Nb, they also exhibit high power factors, as in the previous case, but also high thermal conductivities. Therefore, alloying or nanostructuring have been tried to improve their performance, but not much improvement has been achieved, with the best results obtained at 650 K with a  $zT$  of 0.33.<sup>[196]</sup> This value was later improved by hafnium doping, with values of  $zT$  of 1.47 at 1200 K reported in 2015<sup>[197]</sup> and 1.6 at 1200 K for a solid solution of an alloy  $\text{NbFeSb}$  with Ta, published in 2018.<sup>[198]</sup>

Another interesting family of earth-abundant HH compounds is the one called half-metallic Heusler, such as  $\text{Fe}_2\text{VAl}$  based, where different doping can induce  $n$ - or  $p$ -type semiconductor behavior. For the moment, low  $zT$  values have been reported, due to the high thermal conductivity that they exhibit, but they are promising for low-temperature applications, and thus the research in these materials is still ongoing.<sup>[7,199]</sup> A summary of the best-reported  $zT$  can be found in **Figure 12** for HH materials.

Given that HH compounds contain elements with high melting points (over 1700 K, such as Hf, Zr, Ni, Co, or Ti) along with others with relatively low melting points (Sn, 505 K), high-temperature alloying methods are usually necessary, such as arc-melting in Ar atmosphere,<sup>[200]</sup> inductive heating,<sup>[201]</sup> solid-state reaction,<sup>[198]</sup> melt spinning,<sup>[202]</sup> or SPS.<sup>[203]</sup> In most cases, additional thermal treatments at high temperatures (over 1100 K) for several days followed by rapid quenching are required to obtain pure phases.

As it has been shown in the previous sections, the research on HH materials is quite active and it holds the promise of substituting scarce and toxic materials for low-temperature applications with environmentally friendly, available, and low-cost materials. There was an enterprise, Evident Thermoelectric,

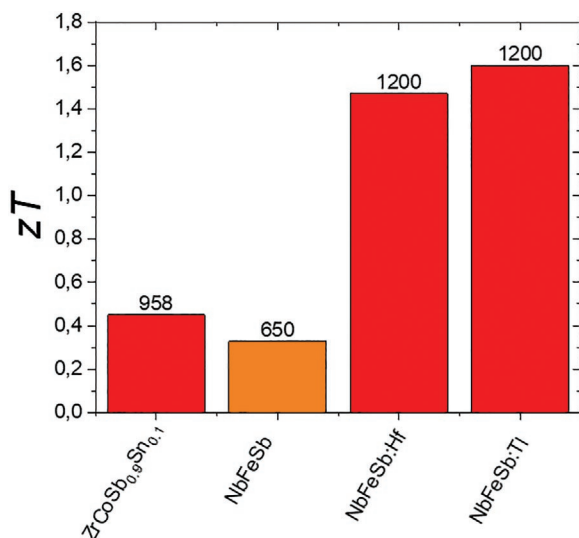


**Figure 12.** Summary of the highest reported  $zT$  values in HH materials (references available in Section 7), maximum  $zT$  value temperatures are indicated in the label. Red represents temperatures above 700 K, and orange is  $zT$  in the medium range temperatures, from 400 to 700 K.

which developed two generators based on HH materials, TEG-HH-8 and TEG-HH-15, which could produce 7.2 and 15 W respectively when a temperature gradient of 500 K was applied.<sup>[109]</sup> In addition, automotive applications with HH materials have been reported, with nearly 50 W produced when the exhaust gas temperature is 600 °C.<sup>[204]</sup>

## 7. Other Eco-Friendly Thermoelectric Materials

Finally, other Eco-Friendly thermoelectric materials can be found among conventional inorganic compounds that have high power factors but also high thermal conductivity. As it is already assumed by the community, nanostructuring can help to reduce the thermal conductivity while still maintaining the power factor, if performed correctly. For instance, 2D structures, obtained from delamination of layered materials such as layered sulfides or layered oxides are demonstrating great capacities for thermoelectric applications, reducing the thermal conductivity due to the reduced dimension and, even presenting an enhancement of the power factor due to quantum confinement.<sup>[28,29,205]</sup> Other forms of nanostructuring materials result in more conventional but eco-friendly semiconductors are being revisited for thermoelectric applications recently. The effect of nanostructuring in semiconductors is shown for instance, in our work with CuNi,<sup>[206]</sup> where through nanostructuring the material, fairly good thermoelectric properties are achieved. Also through nanostructuring, the properties of Silicon, which is a very poor thermoelectric material in its bulk form, can be enhanced. And, they are very attractive given their industrial use in microelectronic applications and their easy integration, many works are dealing with both silicon Si,<sup>[37,207,208,23]</sup> or silicon-based materials, as SiGe alloys,<sup>[209,210]</sup> to cite some recent reviews. In detail, we will briefly comment here on two other types of materials that are being also explored

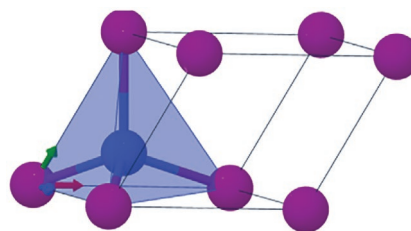


**Figure 13.** A possible crystalline structure of CuI. Here, the Zincblende, Sphalerite structure is represented. Cu<sup>1+</sup> in blue is bound to four equivalents I<sup>1-</sup> atoms, shown in purple, to form corner-sharing CuI<sub>4</sub> tetrahedra.

for thermoelectric applications and have eco-friendly and non-toxicity properties which are the focus of this review.

### 7.1. Copper Iodide

Copper iodide (CuI) is a novel thermoelectric material that presents, apart from a large thermoelectric figure of merit and high Seebeck coefficient, the advantage of being optically transparent in the visible range of the spectrum. CuI (see **Figure 13**) was theoretically predicted based on the Boltzmann transport theory combining, with first-principle calculations, a maximum Seebeck coefficient of  $\approx 250 \mu\text{V} \cdot \text{K}^{-1}$  and a carrier concentration of  $\approx 1020 \text{ cm}^{-3}$  by Yadav and Sanyal in 2014.<sup>[211]</sup> The fabrication of CuI took place over the following years by different groups.<sup>[212–215]</sup> This is the most efficient transparent thermoelectric to date. It behaves as an intrinsically direct p-type semiconductor because of the presence of copper vacancies and the small effective mass ( $0.30 m_0$ ) of the light holes. It presents a high bandgap  $E_g = 3.1 \text{ eV}$  and a large exciton binding energy of 62 meV similar to that of ZnO, as described in the oxide section of this review.

Regarding the thermoelectric properties, the best values so far have been obtained by Faustino et al.<sup>[216]</sup> who reported a power factor of  $4.76 \times 10^{-4} \text{ W} \cdot \text{m}^{-1} \cdot \text{K}^{-2}$  with a  $zT \approx 0.22$  in films prepared by solid iodization. The high values of  $zT$  for this material have been explained by the energy filtering of charge carriers at the interface and grain boundaries allowed only high-energy holes to transfer through the energy barriers, resulting in large Seebeck coefficients. This, combined with a decrease in the charge carrier density, resulted in an increase in the Seebeck coefficient in polycrystalline  $\gamma\text{CuI}$  films.<sup>[217]</sup> So far, high-quality polycrystalline CuI films have been produced using different deposition techniques up to now, such as sputtering,<sup>[218,219]</sup> solid and vapor iodization,<sup>[220,221]</sup> and thermal evaporation.<sup>[222,223]</sup>

Due to their high transparency in the visible range of the spectra this thermoelectric material is very interesting for the development of energy harvesting in smart windows for its transparency and wearable devices given its flexibility.<sup>[212]</sup>

### 7.2. Nitrides

Among the nitride family, different materials have been studied for thermoelectric applications, among which Boron Nitride (BN) based and III-Nitrides (which consist of GaN and its alloys

with Al and In) are the most relevant when earth-abundant elements are taken into account. Boron nitride-based materials are being thoroughly investigated lately, being firstly synthesized in 1842. From the graphene analog of hexagonal boron nitride (h-BN) to boron nitride allotropes and 2D nanostructures have been proposed for thermoelectric applications. A review of these materials and their thermal transport properties can be found in.<sup>[224]</sup> In the case of III-Nitrides, they exhibit a hexagonal wurtzite structure in most cases, and sometimes a zinc blende one. They have a direct bandgap that can be tuned from 0.7 eV (InN) to 6.2 eV (AlN). Also, they can be structured in 2D structures, such as  $B_{1-x}Al_xN$ ,  $Al_{1-x}Ga_xN$ , or  $Ga_{1-x}In_xN$ .<sup>[225]</sup>

Nitrides in general have high electron mobility and thermal stability. Their applications include light-emitting diodes, thanks to their wide direct bandgap range, solar cells, electronics, and RF applications, magnetism, nuclear detection, and thermoelectric generation. A review of III-Nitrides and their applications can be found in references.<sup>[226,227]</sup>

III-Nitrides have a high Seebeck coefficient, being the highest reported value  $500 \mu V \cdot K^{-1}$  for a thin film of GaN with low carrier concentration<sup>[228]</sup> and as it was already said, they are stable in temperature thanks to their wide bandgaps, and therefore, they are interesting candidates for high-temperature applications.<sup>[226]</sup> AlN and InN have been less studied for thermoelectric applications, with the highest theoretically predicted  $zT$  of 1.6 for an InN nanowire at 1000 K.<sup>[229]</sup> In the case of BN, most of the thermoelectric properties have been studied theoretically.<sup>[225]</sup>

Fabrication of GaN epitaxial layers by hydride vapor phase epitaxy,<sup>[228]</sup> or metal-organic vapor deposition have been reported.<sup>[228,230]</sup> In the case of BN, h-BN can be obtained by mechanical exfoliation or chemical vapor deposition, for instance.<sup>[231]</sup>

Most of the work developed to date on thermoelectric devices based on nitrides has been conducted on GaN. For instance, some works are reporting the fabrication of devices consisting of GaN epitaxial layers for their integration in chips with a maximum output power of  $3.35 \times 10^{-6}$  W with 153 K of thermal gradient<sup>[232]</sup> or of 25 p-n pairs to obtain a maximum power of  $2.1 \mu V$  with a gradient temperature of 30 K.<sup>[230]</sup>

## 8. Conclusions and Prospects

Over the last decades, it has been gaining importance the use of materials based on earth-crust abundant, cost-efficient, and sustainable elements that are competitive for thermoelectric applications. To this end, numerous groups are focusing their research on the synthesis and characterization of such compounds. As we have seen, this is being reflected in a drastic increase of publications in sustainable thermoelectric materials. Of these abundant and sustainable elements, sulfur, oxygen, and silicon, and their related-based compounds are the heart of this review. They have a well-established extraction process, developed over many decades, and some of them can be found in minerals, occurring naturally. Moreover, those elements give rise to an enormous variety of compounds that could be synthesized on different architectures and dimensionalities: from bulk to films, layered materials, 2D structures, etc., which could be adapted to a variety of applications.

Regarding sulfides, different binary sulfides such as CuS have been revisited recently for thermoelectric applications, and the figure the merit has been drastically improved. Indicating that when the effort is set on a material the community has the tools and the knowledge to improve it. The principal breakthrough in this field was the discovery of a new phenomenology, the ion-liquid conductivity. Besides, unexplored families such as sulfides perovskites, layered sulfides, or even copper-based sulfides, provide an optimistic future to this family. This together with the fact that the community is progressively gaining expertise in building and designing sulfides based-modules, opens the door to new devices based on these materials in the future. Tetrahedrites may be also considered along with sulfides, occurring as a natural mineral and exhibiting a higher figure of merit than those found on sulfides.

Oxides are a family that has been well investigated in other fields, and which have already been used in thermoelectric prototypes, such as manganese oxide, with high reliability. However, their figure of merit is still low for massive implementation. Non-stoichiometric cobalt oxide thermoelectrics have been theoretically predicted to present better properties when compared to what is already obtained due to their strong anisotropy. This is a promising pathway to the near-future developments in thermoelectricity. Finally, silicides are an archetypic example of success in sustainable thermoelectric compounds, which have already been studied over several decades. Particularly,  $Mg_2Si$  shows a high figure of merit, around 1, and it is widely used at moderate temperatures in several applications. Research into this material is currently focused on increasing the operating temperature and on its mechanical stability. To this end, several attempts are being investigated to overcome these problems. For instance, by doping with elements such as Al or Sn, or using less brittle silicides, respectively.

**Table 1** collects a general summary of the actual performance of the discussed materials, not only as their efficiency is concerned, but also taking into account their sustainability, versatility, and implementation feasibility. In this context, whereas sulfides and tetrahedrites seem to be two excellent families to be used near room temperature, oxides and silicides are preferred to be used at higher temperatures, due to their stability. In terms of synthesis and efficiency, sulfides can be easily synthesized (and their production is scalable) in many structures and morphologies, but they still exhibit low-efficiency values. Tetrahedrites have a high figure of merit, but their synthesis seems to be much more complex than those shown by sulfides. Finally, oxides and silicides exhibit certain difficulties in their synthesis, but some of the oxides show  $zT$  values relatively high. Moreover, some silicides are being already used in high-temperature devices.

In conclusion, there is still much work to be done in the field of sustainable thermoelectric materials, but the current prospective indicates that we are at the starting point to guarantee a smooth transition to sustainable thermoelectricity in the near future. As it has been seen, there is a wide variety of materials with promising thermoelectric properties which could be synthesized (and in a scalable way) with a bunch of well-established (and cost-efficient) methods. Furthermore, their figures of merit could be further improved by using the knowledge already acquired in more traditional thermoelectrics such

**Table 1.** Current feasibility of different materials. Color code: green (fairly conditions), yellow (middle), and red (hard applicable).

Materials	Characteristics				General comments
	Sustainability	Versatility	Efficiency	Implementation feasibility	
Sulfides	Green	Green	Red	Yellow	High number of low-cost, abundant, and versatile compounds. Easy synthesis Low ZT. Utilization recommendable at low T. They hardly have been implemented
Tetrahedrites	Green	Yellow	Green	Green	Long known materials, based on natural minerals. Complex synthesis, High zT at room-medium T.
Oxides	Green	Green	Yellow	Yellow	High number of low-cost, abundant, and versatile compounds Easy synthesis Moderate performance for a large range of temperatures (from 100 to 1250 K)
Half-Heuser alloys	Yellow	Yellow	Green	Yellow	Relative sustainability. High-temperature synthesis. Very high performance for high temperatures (>800 K)
Silicides	Yellow	Yellow	Yellow	Yellow	Complex synthesis. High performance for high temperatures (>600 K)

as doping, nanostructuring, resonant levels, crystallographic anisotropy, preparation methods, band theory, etc. In short, a reshaping of the thermoelectric materials landscape towards a more eco-friendly scenery is plausible to be implemented along this decade, enhancing the global efficiency of the different energy conversion systems and being a more important piece of the green energy deal.

## Acknowledgements

O.C.-C. and M.M.-G. would like to acknowledge financial support from MAT2017-86450-C4-3-R and the 2D\_MESES project from CSIC, and J.R.A., from RTI2018-099794-B-I100.

## Conflict of Interest

The authors declare no conflict of interest.

## Keywords

energy conversion, functional materials, sustainable, thermoelectrics

Received: March 30, 2021

Revised: May 21, 2021

Published online: June 16, 2021

- [1] H. Huang, Y. Cui, Qi Li, C. Dun, W. Zhou, W. Huang, L. Chen, C. A. Hewitt, D. L. Carroll, *Nano Energy* **2016**, 26, 172.
- [2] C. Wan, X. Gu, F. Dang, T. Itoh, Y. Wang, H. Sasaki, M. Kondo, K. Koga, K. Yabuki, G. J. Snyder, R. Yang, K. Koumoto, *Nat. Mater.* **2015**, 14, 622.
- [3] C. S. Matthes, et al. In *2018 IEEE Aerospace Conference*, IEEE, Piscataway, NJ **2018**.
- [4] *Powerwatch*, <https://www.powerwatch.com/> (accessed: February 2021).
- [5] *Tegmart*, <https://www.tegmart.com/wood-stove-thermoelectric-generators/> (accessed: February 2021).

- [6] M. Martín-González, O. Caballero-Calero, P. Díaz-Chao, *Renewable Sustainable Energy Rev.* **2013**, 24, 288.
- [7] D. Beretta, N. Neophytou, J. M. Hodges, M. G. Kanatzidis, D. Narducci, M. Martin-Gonzalez, M. Beekman, B. Balke, G. Cerretti, W. Tremel, A. Zevalkink, A. I. Hofmann, C. Müller, B. Döring, M. Campoy-Quiles, M. Caironi, *Mater. Sci. Eng., R* **2019**, 138, 100501.
- [8] L. D. Hicks, M. S. Dresselhaus, *Phys. Rev. B* **1993**, 47, 12727.
- [9] F. Domínguez-Adame, M. Martín-González, D. Sánchez, A. Cantarero, *Phys. E* **2019**, 113, 213.
- [10] C. V. Manzano, M. Martin-Gonzalez, *Front. Chem.* **2019**, 7, 516.
- [11] J. R. Rumble, D. R. Lide, T. J. Bruno, *CRC handbook of chemistry and physics*, CRC Press, Boca Raton, FL **2018**.
- [12] Md. N. Hasan, H. Wahid, N. Nayan, M. S. Mohamed Ali, *Int. J. Energy Res.* **2020**, 44, 6170.
- [13] R. Freer, A. V. Powell, *J. Mater. Chem. C* **2020**, 8, 441.
- [14] J. J. G. Moreno, et al., *Mater. Renewable Sustainable Energy* **2020**, 9, 16.
- [15] A. V. Powell, *J. Appl. Phys.* **2019**, 126, 100901.
- [16] G. Guélou, et al., *J. Mater. Chem. C* **2021**, 9, 773.
- [17] R. Prasad, S. D. Bham, *Mater. Renewable Sustainable Energy* **2020**, 9, 3.
- [18] N. Baghdadi, N. Salah, A. Alshahrie, A. R. Ansari, K. Koumoto, *Ceram. Int.* **2021**, 47, 6169.
- [19] I. Pallecchi, N. Manca, B. Patil, L. Pellegrino, D. Marré, *Nano Futures* **2020**, 4, 032008.
- [20] W.-Di Liu, L. Yang, Z.-G. Chen, J. Zou, *Adv. Mater.* **2020**, 32, 1905703.
- [21] T. Wang, T. Huo, H. Wang, C. Wang, *Sci. China Mater.* **2020**, 63, 8.
- [22] P.-An Zong, J. Liang, P. Zhang, C. Wan, Y. Wang, K. Koumoto, *ACS Appl. Energy Mater.* **2020**, 3, 2224.
- [23] K. Ziouche, I. Bel-Hadj, Z. Bougrioua, *Nano Energy* **2021**, 80, 105553.
- [24] C. Ou, A. L. Sangle, A. Datta, Q. Jing, T. Busolo, T. Chalklen, V. Narayan, S. Kar-Narayan, *ACS Appl. Mater. Interfaces* **2018**, 10, 19580.
- [25] N. Nandihalli, C.-J. Liu, T. Mori, *Nano Energy* **2020**, 105186.
- [26] T. G. Novak, K. Kim, S. Jeon, *Nanoscale* **2019**, 11, 19684.
- [27] F. F. Jaldurgam, Z. Ahmad, F. Touati, *Nanomaterials* **2021**, 11, 895.
- [28] M. Samanta, T. Ghosh, S. Chandra, K. Biswas, *J. Mater. Chem. A* **2020**, 8, 12226.
- [29] K. Kanahashi, J. Pu, T. Takenobu, *Adv. Energy Mater.* **2020**, 10, 1902842.
- [30] D. Li, et al., *Nano-Micro Lett.* **2020**, 12, 1.

- [31] A. Nozariasmarz, H. Collins, K. Dsouza, M. H. Polash, M. Hosseini, M. Hyland, J. Liu, A. Malhotra, F. M. Ortiz, F. Mohaddes, V. P. Ramesh, Y. Sargolzaeiaval, N. Snouwaert, M. C. Öztürk, D. Vashae, *Appl. Energy* **2020**, *258*, 114069.
- [32] X. Zhu, Y. Yu, F. Li, *Constr. Build. Mater.* **2019**, *228*, 116818.
- [33] N. Jaziri, et al., *Energy Rep.* **2020**, *6*, 264.
- [34] J. Yan, X. Liao, D. Yan, Y. Chen, *J. Microelectromech. Syst.* **2018**, *27*, 1.
- [35] C. C. Yang, S. Li, *ChemPhysChem* **2011**, *12*, 3614.
- [36] N. Neophytou, *Eur. Phys. J. B* **2015**, *88*, 86.
- [37] A. Morata, M. Pacios, G. Gadea, C. Flox, D. Cadavid, A. Cabot, A. Tarancón, *Nat. Commun.* **2018**, *9*, 4759.
- [38] T. Seebeck, *Abh. Dtsch. Akad. Wiss. Berlin, Math.-Naturwiss. Kl.* **1822**, *265*, 1822.
- [39] M. Telkes, A. Mineralogist, *J. Earth Planetary Mater.* **1950**, *35*, 536.
- [40] K. Kato, Y. Okamoto, J. Morimoto, T. Miyakawa, *J. Mater. Sci. Lett.* **1997**, *16*, 914.
- [41] V. K. Gudelli, V. Kanchana, S. Appalakondaiah, G. Vaitheeswaran, M. C. Valsakumar, *J. Phys. Chem. C* **2013**, *117*, 21120.
- [42] J. M. Clamagirand, J. R. Ares, E. Flores, P. Diaz-Chao, F. Leardini, I. J. Ferrer, C. Sánchez, *Thin Solid Films* **2016**, *600*, 19.
- [43] Y. He, T. Day, T. Zhang, H. Liu, X. Shi, L. Chen, G. J. Snyder, *Adv. Mater.* **2014**, *26*, 3974.
- [44] Z.-H. Ge, Bo-P Zhang, Y.-X. Chen, Z.-X. Yu, Y. Liu, J.-F. Li, *Chem. Commun.* **2011**, *47*, 12697.
- [45] Z.-H. Ge, X. Liu, D. Feng, J. Lin, J. He, *Adv. Energy Mater.* **2016**, *6*, 1600607.
- [46] H. Tang, F.-H. Sun, J.-F. Dong, Asfandiyar, H.-Lu Zhuang, Yu Pan, J.-F. Li, *Nano Energy* **2018**, *49*, 267.
- [47] P. Qiu, X. Shi, L. Chen, *Energy Storage Mater.* **2016**, *3*, 85.
- [48] P. Wyżga, M. Bobnar, C. Hennig, A. Leithe-Jasper, T. Mori, R. Gumeniuk, *Z. Anorg. Allg. Chem.* **2017**, *643*, 858.
- [49] R. Ang, A. U. Khan, N. Tsujii, K. Takai, R. Nakamura, T. Mori, *Angew. Chem.* **2015**, *127*, 13101.
- [50] N. Tsujii, T. Mori, *Appl. Phys. Express* **2013**, *6*, 043001.
- [51] Y. Li, T. Zhang, Y. Qin, T. Day, G. Jeffrey Snyder, X. Shi, L. Chen, *J. Appl. Phys.* **2014**, *116*, 203705.
- [52] J. Li, Q. Tan, J.-F. Li, *J. Alloys Compd.* **2013**, *551*, 143.
- [53] D. Berthebaud, O. I. Lebedev, A. Maignan, *J. Materiomics* **2015**, *1*, 68.
- [54] G. Guélou, A. V. Powell, P. Vaqueiro, *J. Mater. Chem. C* **2015**, *3*, 10624.
- [55] S. O. J. Long, A. V. Powell, P. Vaqueiro, S. Hull, *Chem. Mater.* **2018**, *30*, 456.
- [56] A. Ostovari Moghaddam, A. Shokuhfar, A. Cabot, *J. Alloys Compd.* **2018**, *750*, 1.
- [57] A. Ostovari Moghaddam, A. Shokuhfar, P. Guardia, Yu Zhang, A. Cabot, *J. Alloys Compd.* **2019**, *773*, 1064.
- [58] T. Deng, P. Qiu, T. Xing, Z. Zhou, T.-R. Wei, D. Ren, J. Xiao, X. Shi, L. Chen, *J. Mater. Chem. A* **2021**, *9*, 7946.
- [59] K. Suekuni, F. S. Kim, H. Nishiate, M. Ohta, H. I. Tanaka, T. Takabatake, *Appl. Phys. Lett.* **2014**, *105*, 132107.
- [60] Y. Kikuchi, Y. Bouyrie, M. Ohta, K. Suekuni, M. Aihara, T. Takabatake, *J. Mater. Chem. A* **2016**, *4*, 15207.
- [61] C. Bourgès, Y. Bouyrie, A. R. Supka, R. Al Rahal Al Orabi, P. Lemoine, O. I. Lebedev, M. Ohta, K. Suekuni, V. Nassif, V. Hardy, R. Daou, Y. Miyazaki, M. Fornari, E. Guilmeau, *J. Am. Chem. Soc.* **2018**, *140*, 2186.
- [62] Q. Tan, L.-D. Zhao, J.-F. Li, C.-F. Wu, T.-R. Wei, Z.-B. Xing, M. G. Kanatzidis, *J. Mater. Chem. A* **2014**, *2*, 17302.
- [63] H. Q. Yang, X. Y. Wang, H. Wu, B. Zhang, D. D. Xie, Y. J. Chen, Xu Lu, X. D. Han, L. Miao, X. Y. Zhou, *J. Mater. Chem. C* **2019**, *7*, 3351.
- [64] G. Ding, G. Gao, K. Yao, *Sci. Rep.* **2015**, *5*, 1.
- [65] H. Yanagi, Y. Iguchi, T. Sugiyama, T. Kamiya, H. Hosono, *Appl. Phys. Express* **2016**, *9*, 051201.
- [66] C. W. Dunnill, I. Maclaren, D. H. Gregory, *Nanoscale* **2010**, *2*, 90.
- [67] E. E. Abbott, J. W. Kolis, N. D. Lowhorn, W. Sams, A. Rao, T. M. Tritt, *Appl. Phys. Lett.* **2006**, *88*, 262106.
- [68] H. Imai, Y. Shimakawa, Y. Kubo, *Phys. Rev. B* **2001**, *64*, 241104.
- [69] M. Beaumale, T. Barbier, Y. Bréard, S. Hébert, Y. Kinemuchi, E. Guilmeau, *J. Appl. Phys.* **2014**, *115*, 043704.
- [70] G. Guélou, P. Vaqueiro, J. Prado-Gonjal, T. Barbier, S. Hébert, E. Guilmeau, W. Kockelmann, A. V. Powell, *J. Mater. Chem. C* **2016**, *4*, 1871.
- [71] E. Guilmeau, Y. Bréard, A. Maignan, *Appl. Phys. Lett.* **2011**, *99*, 052107.
- [72] P. Misse, D. Berthebaud, O. Lebedev, A. Maignan, E. Guilmeau, *Materials* **2015**, *8*, 2514.
- [73] S. Mitra, T. Maiti, In *Spark Plasma Sintering of Materials*, Springer, New York **2019**, p. 493.
- [74] H. Wu, Xu Lu, G. Wang, K. Peng, H. Chi, B. Zhang, Y. Chen, C. Li, Y. Yan, L. Guo, C. Uher, X. Zhou, X. Han, *Adv. Energy Mater.* **2018**, *8*, 1800087.
- [75] K. Biswas, Li-D Zhao, M. G. Kanatzidis, *Adv. Energy Mater.* **2012**, *2*, 634.
- [76] Z.-H. Ge, Li-D Zhao, Di Wu, X. Liu, Bo-P Zhang, J.-F. Li, J. He, *Mater. Today* **2016**, *19*, 227.
- [77] Y. Shiraishi, R. Okazaki, H. Taniguchi, I. Terasaki, *Jpn. J. Appl. Phys.* **2015**, *54*, 031203.
- [78] M. Baláz, A. Zorkovská, F. Urakaev, P. Baláz, J. Briančin, Z. Bujňáková, M. Achimovičová, E. Gock, *RSC Adv.* **2016**, *6*, 87836.
- [79] S. Wang, Y. Rong, Ye Fan, M. Pacios, H. Bhaskaran, K. He, J. H. Warner, *Chem. Mater.* **2014**, *26*, 6371.
- [80] Y. Rong, Ye Fan, Ai Leen Koh, A. W. Robertson, K. He, S. Wang, H. Tan, R. Sinclair, J. H. Warner, *Nanoscale* **2014**, *6*, 12096.
- [81] A. N. Macinnes, M. B. Power, A. R. Barron, *Chem. Mater.* **1992**, *4*, 11.
- [82] H. Takaki, K. Kobayashi, M. Shimono, N. Kobayashi, K. Hirose, N. Tsujii, T. Mori, *Appl. Phys. Lett.* **2017**, *110*, 072107.
- [83] A. Nozariasmarz, A. Agarwal, Z. A. Coutant, M. J. Hall, J. Liu, R. Liu, A. Malhotra, P. Norouzzadeh, M. C. Öztürk, V. P. Ramesh, Y. Sargolzaeiaval, F. Suarez, D. Vashae, *Jpn. J. Appl. Phys.* **2017**, *56*, 05DA04.
- [84] R. Chetty, A. Bali, R. C. Mallik, *J. Mater. Chem. C* **2015**, *3*, 12364.
- [85] V. R. Hathwar, et al., *Cryst. Growth Des.* **2019**, *19*, 3979.
- [86] X. Lu, D. T. Morelli, Y. Xia, F. Zhou, V. Ozolins, H. Chi, X. Zhou, C. Uher, *Adv. Energy Mater.* **2013**, *3*, 342.
- [87] T. Barbier, P. Lemoine, S. Gascoin, O. I. Lebedev, A. Kaltzoglou, P. Vaqueiro, A. V. Powell, R. I. Smith, E. Guilmeau, *J. Alloys Compd.* **2015**, *634*, 253.
- [88] R. Chetty, P. K. D. S., G. Rogl, P. Rogl, E. Bauer, H. Michor, S. Suwas, S. Puchegger, G. Giester, R. C. Mallik, *Phys. Chem. Chem. Phys.* **2015**, *17*, 1716.
- [89] P. Vaqueiro, G. Guélou, A. Kaltzoglou, R. I. Smith, T. Barbier, E. Guilmeau, A. V. Powell, *Chem. Mater.* **2017**, *29*, 4080.
- [90] Y. Bouyrie, C. Candolfi, A. Dauscher, B. Malaman, B. Lenoir, *Chem. Mater.* **2015**, *27*, 8354.
- [91] E. Makovicky, *Rev. Mineral. Geochem.* **2006**, *61*, 7.
- [92] K. Suekuni, Y. Tomizawa, T. Ozaki, M. Koyano, *J. Appl. Phys.* **2014**, *115*, 143702.
- [93] Y. Bouyrie, C. Candolfi, V. Ohorodniichuk, B. Malaman, A. Dauscher, J. Tobola, B. Lenoir, *J. Mater. Chem. C* **2015**, *3*, 10476.
- [94] A. P. Gonçalves, et al., *Solid State Phenom.* **2017**, *257*, 135.
- [95] J. Van Ermbden, K. Latham, N. W. Duffy, Y. Tachibana, *J. Am. Chem. Soc.* **2013**, *135*, 11562.
- [96] J. Heo, G. Laurita, S. Muir, M. A. Subramanian, D. A. Keszler, *Chem. Mater.* **2014**, *26*, 2047.
- [97] R. Chetty, A. Bali, M. H. Naik, G. Rogl, P. Rogl, M. Jain, S. Suwas, R. C. Mallik, *Acta Mater.* **2015**, *100*, 266.



- [98] D. S. Prem Kumar, S. Tippireddy, A. Ramakrishnan, K.-H. Chen, P. Malar, R. C. Mallik, *Semicond. Sci. Technol.* **2019**, *34*, 035017.
- [99] X. Lu, D. T. Morelli, Yi Xia, V. Ozolins, *Chem. Mater.* **2015**, *27*, 408.
- [100] Xu Lu, D. Morelli, *J. Electron. Mater.* **2014**, *43*, 1983.
- [101] D. S. Prem Kumar, R. Chetty, O. E. Femi, K. Chattopadhyay, P. Malar, R. C. Mallik, *J. Electron. Mater.* **2017**, *46*, 2616.
- [102] Fu-H Sun, J. Dong, H. Tang, P.-P. Shang, H.-L. Zhuang, H. Hu, C.-F. Wu, Yu Pan, J.-F. Li, *Nano Energy* **2019**, *57*, 835.
- [103] Bo Yang, Q. Wang, H. Guo, X. Yang, D. Yang, *Mater. Res. Express* **2020**, *7*, 105504.
- [104] S. O. Long, A. V. Powell, S. Hull, F. Orlandi, C. C. Tang, A. R. Supka, M. Fornari, P. Vaquero, *Adv. Funct. Mater.* **2020**, *30*, 1909409.
- [105] L. L. Huang, Y. S. Wang, C. Zhu, R. Xu, J. M. Li, J. H. Zhang, D. Li, Z. M. Wang, L. Wang, C. J. Song, H. X. Xin, J. Zhang, X. Y. Qin, *J. Alloys Compd.* **2018**, *769*, 478.
- [106] T. Barbier, S. Rollin-Martinet, P. Lemoine, F. Gascoin, A. Kaltzoglou, P. Vaquero, A. V. Powell, E. Guilmeau, *J. Am. Ceram. Soc.* **2016**, *99*, 51.
- [107] J.-H. Pi, S.-G. Kwak, S.-Y. Kim, G.-E. Lee, I.-H. Kim, *J. Electron. Mater.* **2019**, *48*, 1991.
- [108] X. Lu, D. T. Morelli, *Phys. Chem. Chem. Phys.* **2013**, *15*, 5762.
- [109] D. Champier, *Energy Convers. Manage.* **2017**, *140*, 167.
- [110] Y. Wu, In *Metal Oxides in Energy Technologies.*, Elsevier, New York **2018**.
- [111] I. Terasaki, Y. Sasago, K. Uchinokura, *Phys. Rev. B* **1997**, *56*, R12685.
- [112] B.-R. Chen, et al., *Nat. Commun.* **2018**, *9*, 1.
- [113] C. V. Manzano, D. Alegre, O. Caballero-Calero, B. Alén, M. S. Martín-González, *J. Appl. Phys.* **2011**, *100*, 043538.
- [114] H. Zheng, J. Z. Ou, M. S. Strano, R. B. Kaner, A. Mitchell, K. Kalantar-Zadeh, *Adv. Funct. Mater.* **2011**, *21*, 2175.
- [115] R. B. Darling, S. Iwanaga, *Sadhana* **2009**, *34*, 531.
- [116] K. Koumoto, I. Terasaki, R. Funahashi, *MRS Bull.* **2006**, *31*, 206.
- [117] I. Terasaki, M. Iwakawa, T. Nakano, A. Tsukuda, W. Kobayashi, *Dalton Trans.* **2010**, *39*, 1005.
- [118] I. Terasaki, *J. Appl. Phys.* **2011**, *110*, 053705.
- [119] S. Walia, S. Balendhran, H. Nili, S. Zhuyikov, G. Rosengarten, Q. H. Wang, M. Bhaskaran, S. Sriram, M. S. Strano, K. Kalantar-Zadeh, *Prog. Mater. Sci.* **2013**, *58*, 1443.
- [120] J. W. Fergus, *J. Eur. Ceram. Soc.* **2012**, *32*, 525.
- [121] G. Kieslich, G. Cerretti, I. Veremchuk, R. P. Hermann, M. Panthöfer, J. Grin, W. Tremel, *Phys. Status Solidi A* **2016**, *213*, 808.
- [122] I. Tsuyumoto, T. Hosono, M. Murata, *J. Am. Ceram. Soc.* **2006**, *89*, 2301.
- [123] J. Tang, et al., *J. Phys.: Condens. Matter* **2009**, *21*, 205703.
- [124] L. Miao, et al., *ACS Appl. Mater. Interfaces* **2010**, *2*, 2355.
- [125] P. Thiel, J. Eilertsen, S. Populoh, G. Saucke, M. Döbeli, A. Shkabko, L. Sagarna, L. Karvonen, A. Weidenkaff, *J. Appl. Phys.* **2013**, *114*, 243707.
- [126] M. H. Zirin, D. Trivich, *J. Chem. Phys.* **1963**, *39*, 870.
- [127] C. Abinaya, K. Bethke, V. Andrei, J. Baumann, B. Pollakowski-Herrmann, B. Kanngießner, B. Beckhoff, G. C Vázquez, J. Mayandi, T. G. Finstad, K. Rademann, *RSC Adv.* **2020**, *10*, 29394.
- [128] A. Serrano, O. Caballero-Calero, M. Á. García, Šž Lazić, N. Carmona, G. R. Castro, M. Martín-González, J. F. Fernández, *J. Eur. Ceram. Soc.* **2020**, *40*, 5535.
- [129] F. Rubio-Marcos, C. V. Manzano, J. J. Reinoso, I. Lorite, J. J. Romero, J. F. Fernández, M. S. Martín-González, *J. Alloys Compd.* **2011**, *509*, 2891.
- [130] C. V. Manzano, D. Alegre, O. Caballero-Calero, B. Alén, M. S. Martín-González, *J. Appl. Phys.* **2011**, *110*, 043538.
- [131] K. P. Ong, D. J. Singh, P. Wu, *Phys. Rev. B* **2011**, *83*, 115110.
- [132] T. Tsubota, M. Ohtaki, K. Eguchi, H. Arai, *J. Mater. Chem.* **1997**, *7*, 85.
- [133] S. Saini, P. Mele, H. Honda, K. Matsumoto, K. Miyazaki, A. Ichinose, *J. Electron. Mater.* **2014**, *43*, 2145.
- [134] J. Mayandi, R. K. Madathil, C. Abinaya, K. Bethke, V. Venkatachalapathy, K. Rademann, T. Norby, T. G. Finstad, *Mater. Lett.* **2021**, 129352.
- [135] R. Zahra, K. Mahmood, A. Ali, U. Rehman, N. Amin, M. I. Arshad, S. Hussain, M. H. R. Mahmood, *Ceram. Int.* **2019**, *45*, 312.
- [136] H. Colder, E. Guilmeau, C. Harnois, S. Marinel, R. Retoux, E. Savary, *J. Eur. Ceram. Soc.* **2011**, *31*, 2957.
- [137] K.-H. Jung, K. Hyoung Lee, W.-S. Seo, S.-M. Choi, *Appl. Phys. Lett.* **2012**, *100*, 253902.
- [138] M. Ohtaki, K. Araki, K. Yamamoto, *J. Electron. Mater.* **2009**, *38*, 1234.
- [139] F. Kaiser, M. Schmidt, Y. Grin, I. Veremchuk, *Chem. Mater.* **2020**, *32*, 2025.
- [140] F. Kaiser, P. Simon, U. Burkhardt, B. Kieback, Y. Grin, I. Veremchuk, *Crystals* **2017**, *7*, 271.
- [141] M. Liu, B. Su, Y. Tang, X. Jiang, A. Yu, *Adv. Energy Mater.* **2017**, *7*, 1700885.
- [142] M. Shikano, R. Funahashi, *Appl. Phys. Lett.* **2003**, *82*, 1851.
- [143] W. Koshibae, K. Tsutsui, S. Maekawa, *Phys. Rev. B* **2000**, *62*, 6869.
- [144] E. Ermawan, S. Poertagji, *Int. J. Eng. Technol.* **2015**, *15*, 42.
- [145] Y. Takashima, Yu-Q Zhang, J. Wei, B. Feng, Y. Ikuhara, H. J. Cho, H. Ohta, *J. Mater. Chem. A* **2021**, *9*, 274.
- [146] H. Ohta, K. Sugiura, K. Koumoto, *Inorg. Chem.* **2008**, *47*, 8429.
- [147] R. Funahashi, I. Matsubara, H. Ikuta, T. Takeuchi, U. Mizutani, S. Sodeoka, *Jpn. J. Appl. Phys.* **2000**, *39*, L1127.
- [148] G. J. Snyder, E. S. Toberer, *Nat. Mater.* **2008**, *7*, 105.
- [149] N. Baghdadi, N. Salah, A. Alshahrie, K. Koumoto, *Crystals* **2020**, *10*, 610.
- [150] S. Mullenko In *Fundamentals of Laser-Assisted Micro-and Nanotechnologies 2010*, SPIE, Bellingham, WA **2011**.
- [151] H. Ikeda, *J. Phys.: Conf. Ser.* **2018**, *1052*, 012017.
- [152] A. Ghods, C. Zhou, I. T. Ferguson, *J. Vac. Sci. Technol., A* **2020**, *38*, 042408.
- [153] L. W. Guo, D. L. Peng, H. Makino, T. Hanada, S. K. Hong, K. Sumiyama, T. Yao, K. Inaba, *J. Appl. Phys.* **2001**, *90*, 351.
- [154] D. Kurita, et al., *J. Appl. Phys.* **2006**, *100*, 096105.
- [155] TECTEG. *Calcium/Manganese (CMO) TEG modules*, <https://tecteg.com/cmo-oxide-cmo-cascade-800c-hot-side-thermoelectric-power-modules/> (accessed: 2021).
- [156] E. Nikitin, *Sov. Phys. Tech. Phys* **1958**, *3*, 20.
- [157] W. Liu, K. Yin, Q. Zhang, C. Uher, X. Tang, *Natl. Sci. Rev.* **2017**, *4*, 611.
- [158] W. Luo, H. Li, Y. Yan, Z. Lin, X. Tang, Q. Zhang, C. Uher, *Intermetallics* **2011**, *19*, 404.
- [159] K. Kondoh, H. Ogino, E. Yuasa, T. Aizawa, *Mater. Trans.* **2001**, *42*, 1293.
- [160] C. B. Vining, *CRC Handb. Thermoelectr.* **1995**, *1*, 329.
- [161] Y. Miyazaki, D. Igarashi, K. Hayashi, T. Kajitani, K. Yubuta, *Phys. Rev. B* **2008**, *78*, 214104.
- [162] E. Groß, M. Riffel, U. Stöhrer, *J. Mater. Res.* **1995**, *10*, 34.
- [163] M. I. Fedorov, V. K. Zaitsev, G. N. Isachenko, *Solid State Phenomena* **2011**, *170*, 286.
- [164] N. Mingo, D. Hauser, N. P. Kobayashi, M. Plissonnier, A. Shakouri, *Nano Lett.* **2009**, *9*, 711.
- [165] Q. R. Hou, Z. M. Wang, Y. J. He, *Appl. Phys. A Mater. Sci. Process.* **2005**, *80*, 1807.
- [166] H. Liu, G. She, X. Huang, X. Qi, L. Mu, X. Meng, W. Shi, *J. Phys. Chem. C* **2013**, *117*, 2377.
- [167] J. M. Higgins, A. L. Schmitt, I. A. Guzei, S. Jin, *J. Am. Chem. Soc.* **2008**, *130*, 16086.
- [168] T. Itoh, M. Yamada, *J. Electron. Mater.* **2009**, *38*, 925.
- [169] A. J. Zhou, T. J. Zhu, X. B. Zhao, S. H. Yang, T. Dasgupta, C. Stiewe, R. Hassdorf, E. Mueller, *J. Electron. Mater.* **2010**, *39*, 2002.

- [170] A. J. Zhou, X. B. Zhao, T. J. Zhu, S. H. Yang, T. Dasgupta, C. Stiewe, R. Hassdorf, E. Mueller, *Mater. Chem. Phys.* **2010**, *124*, 1001.
- [171] W. Luo, H. Li, F. Fu, W. Hao, X. Tang, *J. Electron. Mater.* **2011**, *40*, 1233.
- [172] Wu Li, L. Lindsay, D. A. Broido, D. A. Stewart, N. Mingo, *Phys. Rev. B* **2012**, *86*, 174307.
- [173] S.-W. You, K.-H. Park, I.-H. Kim, S.-M. Choi, W.-S. Seo, S.-U. Kim, *J. Electron. Mater.* **2012**, *41*, 1675.
- [174] M. Ioannou, G. Polymeris, E. Hatzikraniotis, A. U. Khan, K. M. Paraskevopoulos, Th. Kyratsi, *J. Electron. Mater.* **2013**, *42*, 1827.
- [175] S. Battiston, S. Fiameni, M. Saleemi, S. Boldrini, A. Famengo, F. Agresti, M. Stingaciu, M. S. Toprak, M. Fabrizio, S. Barison, *J. Electron. Mater.* **2013**, *42*, 1956.
- [176] A. Nozariasbmarz, P. Roy, Z. Zamanipour, J. H Dycus, M. J. Cabral, J. M. Lebeau, J. S. Krasinski, D. Vashae, *APL Mater.* **2016**, *4*, 104814.
- [177] Y. Gelbstein, J. Tunbridge, R. Dixon, M. J. Reece, H. Ning, R. Gilchrist, R. Summers, I. Agote, M. A. Lagos, K. Simpson, C. Rouaud, P. Feulner, S. Rivera, R. Torrecillas, M. Husband, J. Crossley, I. Robinson, *J. Electron. Mater.* **2014**, *43*, 1703.
- [178] S.-J. Joo, Ho S Lee, Ji E Lee, J. Jang, *J. Alloys Compd.* **2018**, *747*, 603.
- [179] R. D. Schmidt, E. D. Case, J. Giles, J. E. Ni, T. P. Hogan, *J. Electron. Mater.* **2012**, *41*, 1210.
- [180] Q. Zhang, X. B. Zhao, H. Yin, T. J. Zhu, *J. Alloys Compd.* **2008**, *464*, 9.
- [181] M. Iida, T. Nakamura, K. Fujimoto, Y. Yamaguchi, R. Tamura, T. Iida, K. Nishio, *MRS Adv.* **2016**, *1*, 3971.
- [182] J. Schilz, M. Riffel, K. Pixius, H.-J. Meyer, *Powder Technol.* **1999**, *105*, 149.
- [183] H. J. Lee, Y. R. Cho, I.-H. Kim, *J. Ceramic Process. Res.* **2011**, *12*, 16.
- [184] S. C. Zhou, C. G. Bai, C. L. Fu, *Adv. Mater. Res.* **2011**, *197–198*, 417.
- [185] M. Akasaka, T. Iida, T. Nemoto, J. Soga, J. Sato, K. Makino, M. Fukano, Y. Takanaishi, *J. Cryst. Growth* **2007**, *304*, 196.
- [186] G. Kim, H. Lee, J. Kim, J. W. Roh, I. Lyo, B.-W. Kim, K. H. Lee, W. Lee, *Scr. Mater.* **2017**, *128*, 53.
- [187] V. Zaitsev, et al., In *Thermoelectrics Handbook: Macro to Nano*, (Ed: DM Rowe), CRC Press Taylor & Francis, Boca Raton, FL **2006**, p. 29.
- [188] V. Zaitsev, et al., In *Twenty-First International Conference on Thermoelectrics, 2002, Proceedings ICT'02*, IEEE, Piscataway, NJ **2002**.
- [189] M. I. Fedorov, V. K. Zaitsev, I. S. Eremin, E. A. Gurieva, A. T. Burkov, P. P. Konstantinov, M. V. Vedernikov, A. Yu. Samunin, G. N. Isachenko, A. A. Shabaldin, *Phys. Solid State* **2006**, *48*, 1486.
- [190] Y. Miyazaki, Y. Kikuchi, *Springer Series in Material Science, Vol.182*, Springer, New York **2013**.
- [191] S. Ghodke, N. Hiroishi, A. Yamamoto, H. Ikuta, M. Matsunami, T. Takeuchi, *J. Electron. Mater.* **2016**, *45*, 5279.
- [192] G. Samsonov, G. Samsonov, *Plenum Press Handbook of High-Temperature Materials*, Plenum Press, Springer, Germany **1964**.
- [193] U. Gottlieb, B. Lambert-Andron, F. Nava, M. Affronte, O. Laborde, A. Rouault, R. Madar, *J. Appl. Phys.* **1995**, *78*, 3902.
- [194] Y. Sakamaki, et al., *MRS Online Proc. Libr.* **2003**, *753*, 1777.
- [195] S. Sakurada, N. Shutoh, *Appl. Phys. Lett.* **2005**, *86*, 082105.
- [196] T. Sekimoto, K. Kurosaki, H. Muta, S. Yamanaka, *Jpn. J. Appl. Phys.* **2007**, *46*, L673.
- [197] C. Fu, et al., *Nat. Commun.* **2015**, *6*, 1.
- [198] J. Yu, C. Fu, Y. Liu, K. Xia, U. Aydemir, T. C. Chasapis, G. J. Snyder, X. Zhao, T. Zhu, *Adv. Energy Mater.* **2018**, *8*, 1701313.
- [199] L. Huang, Q. Zhang, Bo Yuan, X. Lai, X. Yan, Z. Ren, *Mater. Res. Bull.* **2016**, *76*, 107.
- [200] F. Serrano-Sánchez, T. Luo, J. Yu, W. Xie, C. Le, G. Auffermann, A. Weidenkaff, T. Zhu, X. Zhao, J. A. Alonso, B. Gault, C. Felser, C. Fu, *J. Mater. Chem. A* **2020**, *8*, 14822.
- [201] Y. Xing, R. Liu, Yi-Y Sun, F. Chen, K. Zhao, T. Zhu, S. Bai, L. Chen, *J. Mater. Chem. A* **2018**, *6*, 19470.
- [202] C. Yu, et al., *J. Electron. Mater.* **2010**, *39*, 2008.
- [203] N. S. Chauhan, S. Bathula, A. Vishwakarma, R. Bhardwaj, K. Kumar Johari, B. Gahtori, A. Dhar, *Mater. Lett.* **2018**, *228*, 250.
- [204] J. Szybist, et al., *Performance of a Half-Heusler Thermoelectric Generator for Automotive Application*, No. 2018-01-0054, SAE Technical Paper **2018**.
- [205] Y.-Y. Liu, et al., *J. Phys.: Condens. Matter* **2018**, *30*, 275701.
- [206] C. V. Manzano, et al., *J. Mater. Chem. C* **2021**, *9*, 3447.
- [207] G. Gadea Díez, J. M. Sojo Gordillo, M. Pacios Pujadó, M. Salleras, L. Fonseca, A. Morata, A. Tarancón Rubio, *Nano Energy* **2020**, *67*, 104191.
- [208] S. Elyamny, E. Dimaggio, S. Magagna, D. Narducci, G. Pennelli, *Nano Lett.* **2020**, *20*, 4748.
- [209] J. A. Perez-Taborda, M. Muñoz Rojo, J. Maiz, N. Neophytou, M. Martin-Gonzalez, *Sci. Rep.* **2016**, *6*, 32778.
- [210] I. Donmez Noyan, G. Gadea, M. Salleras, M. Pacios, C. Calaza, A. Stranz, M. Dolcet, A. Morata, A. Tarancon, L. Fonseca, *Nano Energy* **2019**, *57*, 492.
- [211] M. K. Yadav, B. Sanyal, *Mater. Res. Express* **2014**, *1*, 015708.
- [212] C. Yang, et al., *Nat. Commun.* **2017**, *8*, 1.
- [213] N. P. Klochko, V. R. Kopach, I. I. Tyukhov, G. S. Khrypunov, V. E. Korsun, V. O. Nikitin, V. M. Lyubov, M. V. Kirichenko, O. N. Otchenashko, D. O. Zhadan, M. O. Maslak, A. L. Khrypunova, *Sol. Energy* **2017**, *157*, 657.
- [214] M. Kneiß, C. Yang, J. Barzola-Quiquia, G. Benndorf, H. Von Wenckstern, P. Esquinazi, M. Lorenz, M. Grundmann, *Adv. Mater. Interfaces* **2018**, *5*, 1701411.
- [215] R. Mulla, M. K. Rabinal, *Energy Technol.* **2018**, *6*, 1178.
- [216] B. M. M. Faustino, et al., *Sci. Rep.* **2018**, *8*, 1.
- [217] P. P. Murmu, V. Karthik, Z. Liu, V. Jovic, T. Mori, W. L. Yang, K. E. Smith, J. V. Kennedy, *ACS Appl. Energy Mater.* **2020**, *3*, 10037.
- [218] M. Grundmann, F.-L. Schein, M. Lorenz, T. Böntgen, J. Lenzner, H. Von Wenckstern, *Phys. Status Solidi A* **2013**, *210*, 1671.
- [219] C. Yang, M. Kneiß, M. Lorenz, M. Grundmann, *Proc. Natl. Acad. Sci. U. S. A.* **2016**, *113*, 12929.
- [220] N. Yamada, R. Ino, H. Tomura, Y. Kondo, Y. Ninomiya, *Adv. Electron. Mater.* **2017**, *3*, 1700298.
- [221] S. Gol, R. N. Pena, M. F. Rothschild, M. Tor, J. Estany, *Sci. Rep.* **2018**, *8*, 14336.
- [222] D. K. Kaushik, M. Selvaraj, S. Ramu, A. Subrahmanyam, *Sol. Energy Mater. Sol. Cells* **2017**, *165*, 52.
- [223] F. Geng, L. Yang, B. Dai, S. Guo, G. Gao, L. Xu, J. Han, A. Bolshakov, J. Zhu, *Surf. Coat. Technol.* **2019**, *361*, 396.
- [224] V. Sharma, H. L. Kagdada, P. K. Jha, P. Śpiewak, K. J. Kurzydłowski, *Renewable Sustainable Energy Rev.* **2020**, *120*, 109622.
- [225] D. Wines, F. Ersan, C. Ataca, *ACS Appl. Mater. Interfaces* **2020**, *12*, 46416.
- [226] N. Lu, I. Ferguson, *Semicond. Sci. Technol.* **2013**, *28*, 074023.
- [227] C. Zhou, A. Ghods, V. G. Saravade, P. V. Patel, K. L. Yunghans, C. Ferguson, Y. Feng, B. Kucukgok, N. Lu, I. T. Ferguson, *ECS J. Solid State Sci. Technol.* **2017**, *6*, Q149.
- [228] B. Kucukgok, B. Wang, A. G. Melton, N. Lu, I. T. Ferguson, *Phys. Status Solidi C* **2014**, *11*, 894.
- [229] H.-H. Huang, I.-L. Lu, Y.-R. Wu, *Phys. Status Solidi A* **2011**, *208*, 1562.
- [230] A. Sztejn, H. Ohta, J. Sonoda, A. Ramu, J. E. Bowers, S. P. Denbaars, S. Nakamura, *Appl. Phys. Express* **2009**, *2*, 111003.
- [231] J. Yin, J. Li, Y. Hang, J. Yu, G. Tai, X. Li, Z. Zhang, W. Guo, *Small* **2016**, *12*, 2942.
- [232] N. Kaiwa, M. Hoshino, T. Yaginuma, R. Izaki, S. Yamaguchi, A. Yamamoto, *Thin Solid Films* **2007**, *515*, 4501.
- [233] www.compoundchem.com (accessed: June 2021).



**Olga Caballero-Calero** obtained her Ph.D. in Physics in 2007 at Universidad Autónoma de Madrid (Spain). In the first stages of her career, she worked in Integrated Optics, Astrophysics Instrumentation, and Nanotechnology. She made several stays abroad in renowned international institutes (Boston University, USA and Bonn University, Germany during her Ph.D. and Université de Grenoble, France in a Postdoctoral position). Currently, the main topics of her research are the fabrication of novel thermoelectric devices for the harvesting of wasted heat for its use as electricity, and the study of novel nano-structures of different materials to modify their properties.



**Jose R. Ares** obtained his Ph.D. in Physics in 2002 at Universidad Autónoma de Madrid (Spain). After a first postdoctoral stay at ICMPE/CNRS (France), he moved to a Marie Curie Action postdoctoral position shared between GKSS (Germany) and Oxford University (UK). In 2006, he got a tenure track position (Ramon y Cajal fellowship) in Spain. Since 2012, he is an associate professor at UAM combining academia and research. He is currently the coordinator of a Master's Degree about energy at UAM. His main research activities focus on properties of novel materials for energy storage and conversion, particularly on hydrides and sulfides to be used as hydrogen storage and thermoelectric materials, respectively.



**Marisol Martin-Gonzalez** is heading an interdisciplinary group (FINDER) at the Institute of Micro and Nanotechnology (IMN-CSIC) focused mainly on nanoengineering materials for energy harvesting. She holds a Ph.D. degree since 2000. Afterward, she did her postdoc at U.C. Berkeley. She has been also visiting professor at MIT and RPI. She is the author of more than 130 publications. Regarding technology transfer, she holds five patents and is the co-founder of a spin-off company. She has been elected as part of the European thermoelectric Society board and she became recently the Materials area coordinator at CSIC.